

**Conjugation of anti-CD47 antibody to gold nanoparticles
via click chemistry for cancer therapy**

Brian Christopher Ayers

May 13, 2014

Dr. Jeffrey Byers and Dr. Jeremy Ward

Thesis Advisors

Submitted in the name of Science

in

the Department of Chemistry and Biochemistry

Middlebury College

Approved by:

Jeffrey Byers, Ph.D. (Thesis Advisor)

Jeremy Ward, Ph.D. (Thesis Advisor)

Roger Sandwick, Ph.D.

Honor Code:

I have neither given nor received unauthorized aid in completing this thesis.

Brian Ayers

Abstract

We investigate the conjugation of anti-CD47 monoclonal antibodies to gold nanoparticles via click chemistry for cancer therapy. Anti-CD47 antibody has been demonstrated to both inhibit primary tumor growth as well as tumor metastasis *in vivo*. However, healthy cells also express CD47, making anti-CD47 antibody a nonspecific treatment. Gold nanoparticles (<100 nm) exhibit an enhanced permeability and retention rate (EPR) in tumors, making them an effective directed delivery system for drugs. Dodecanethiolate gold nanoparticles (3 nm) were synthesized and characterized by ^1H NMR spectroscopy and dynamic light scattering. Subsequent bromoundecanethiol exchange was conducted on the dodecanethiolate gold nanoparticles followed by an azide substitution to produce azidoundecanethiolate gold nanoparticles, which were characterized by ^1H NMR spectroscopy and dynamic light scattering. Click chemistry was then utilized to conjugate anti-CD47 antibody to the gold nanoparticles. The efficacy of the conjugation was investigated by an ELISA assay, and found to be insignificant ($p > 0.05$). The anti-CD47-AuNP product from the click chemistry reaction demonstrated no toxicity to *Homo sapiens* lung carcinoma cells *in vitro*. In the future, the efficacy of the click chemistry conjugation will be improved and the therapeutic effect of anti-CD47-AuNP as a cancer therapy will be measured by its ability to induce tumor cell phagocytosis by macrophages. We hypothesize that the directed delivery of the gold nanoparticles will allow the conjugated antibody-nanoparticle drug to show improved effectiveness over the antibody therapy alone in inducing tumor cell death.

Acknowledgements

I want to give special thanks to my two great advisors Jeffrey Byers and Jeremy Ward. I am very thankful for their willingness to support me on an independent project not directly related to their personal research. They in no way had to agree to take on the extra work and time commitment of advising me on this project, and it is only because of their willingness to go above and beyond that I was given this opportunity. They have taught me an incredible amount over the course of the thesis, and it has been the opportunity to work with and get to know them that has made this project such a fun and rewarding experience. Thank you.

I also want to thank Nancy Graham for sharing her lab space with me, putting up with my endless questions about where equipment is located, and for her sense of humor which made working in lab much more enjoyable. Also thank you to Roger Sandwick for being on my thesis committee and helpfulness in advising me on biochemistry topics and techniques.

Thank you to Judy Mayer and Tom Sheluga, without whom I don't think anything in BiHall would be accomplished. Also special thanks to the Undergraduate Research Office, Chemistry Department, and Biology department for providing the funding for this research endeavor.

Finally, thank you to my family and friends. My parents for giving me the opportunity to attend Middlebury College and pursue a field that I love, as well as my friends for supporting me throughout the highs and lows that make up a senior thesis in biochemistry.

Table of Contents

1. Introduction	1
1.1 Cancer By The Numbers	2
1.2 History of Cancer Therapy Approaches	2
1.3 Current Monoclonal Antibody Therapies	4
1.4 CD47 as a Cancer Therapy Target	5
1.5 Nanoparticles as Directed Drug Delivery Systems	7
1.6 Anti-CD47 Conjugated Gold Nanoparticle Therapy	10
2. Materials and Methods	11
2.1 Materials	11
2.2 Dodecanethiolate Gold Nanoparticle Synthesis	11
2.3 Ligand Exchange with Bromoundecanthiol	12
2.4 Azidation of Gold Nanoparticles	12
2.5 Cell Culture Method	12
2.6 Cytotoxicity of Dodecanethiolate and Azidoundecanethiolate Nanoparticles	13
2.7 Azido-PEG-Thiol Gold Nanoparticle Modification	14
2.8 Anti-CD47 Antibody Functionalization	14
2.9 Conjugation of Anti-CD47 to Gold Nanoparticles via Click-Chemistry	14
2.10 ELISA Assay	15
2.11 Anti-CD47-AuNP Cytotoxicity Assay	16
3. Results and Discussion	17
3.1 Dodecanethiolate-Gold Nanoparticle Synthesis	17
3.2 Bromoundecanthiol and Azide Substitutions on Gold Nanoparticles	20
3.4 Thiol-PEG-Azide Nanoparticle Modification and Antibody Functionalization	25
3.5 Conjugation of anti-CD47 antibodies to Gold Nanoparticles via Click Chemistry	27
3.6 Cytotoxicity of Anti-CD47-AuNP Conjugated Final Product	29
3.7 Future Direction.....	30
4. Conclusion	31
5. References.....	32

Table of Figures

Figure 1: Antibody Structure: Variable and Constant Regions	4
Figure 2: Anti-CD47 Therapeutic Effect	5
Figure 3: Normal and Cancerous cell comparison	6
Figure 4: Accumulation of nanoparticles due to EPR	7
Figure 5: EDC coupled reaction mechanism	9
Figure 6: Click Chemistry Reaction mechanism	9
Figure 7: Anti-CD47 Conjugated Gold Nanoparticle Cancer Therapy Drug	10
Figure 8: Synthesis of dodecanethiolate gold nanoparticles	18
Figure 9: ¹ H NMR spectrum of dodecanethiolate-AuNPs	19
Figure 10: Size distribution of dodecanethiolate gold nanoparticles	19
Figure 11: Thiol-ligand exchange of bromoundecanethiol on dodecanethiol AuNP	20
Figure 12: Azide substitution on bromoundecanethiol AuNP	21
Figure 13: ¹ H NMR spectrum of azidoundecanethiolate-AuNPs	22
Figure 14: Size distribution of azidoundecanethiolate gold nanoparticles	22
Figure 15: Cytotoxicity of gold nanoparticles <i>in vitro</i>	24
Figure 16: Thiol-PEG-Azide modification of gold nanoparticles for water solubility	25
Figure 17: Functionalization of anti-CD47 antibody with propargyl-dPEG-NHS ester	26
Figure 18: Amine groups part of antibody structure	26
Figure 19: Click chemistry of alkyne-antibodies with azido-gold nanoparticles	27
Figure 20: ELISA of click chemistry anti-CD47-AuNP conjugation	28
Figure 21: Cytotoxicity of anti-CD47-AuNP <i>in vitro</i>	29

Table of Tables

Table 1: Plate layout of cytotoxicity assay of gold nanoparticles	13
Table 2: Plate layout of anti-CD47 ELISA assay	15
Table 3: Plate layout of cytotoxicity assay of anti-CD47-AuNP final product.....	16

1. Introduction

Monoclonal antibodies are emerging as effective therapeutic cancer drugs because of their potential ability to attack cancerous cells in a highly specific manner.⁵ Antibodies are able to bind with very high specificity to a single antigen target,⁶ such as biomarker proteins expressed by cancer cells.^{7,8} Once bound, antibodies can facilitate the destruction of tumor cells through a number of different mechanisms,⁵ including perturbation of cell signaling,⁹ activation of complement dependent cytotoxicity (CDC),¹⁰ antibody dependent cellular cytotoxicity (ADCC),¹¹ and induction of adaptive immunity.¹²

A promising antibody cancer therapy is anti-CD47.^{13,14} CD47 is an extracellular protein overexpressed by tumor cells as an anti-phagocytic signal.¹⁴ Blocking this signal with anti-CD47 antibody induces tumor-cell phagocytosis, inhibiting both primary tumor growth as well as preventing tumor metastasis.¹³ However, CD47 is also expressed by healthy cells, making anti-CD47 antibody a non-specific cancer treatment as the injected antibody can bind to any cell in the body. This general nature of the treatment reduces the antibody's effectiveness at treating established tumors, as the antibody alone has been shown to be unable to eliminate tumors once they are of a certain threshold size.¹³

Conjugating an antibody to nanoparticles for directed drug delivery is a promising technique for improving the effectiveness of antibody cancer therapy.¹⁵⁻¹⁸ The small size of nanoparticles (<100 nm) allows them to pass through the larger pores of the "leaky" tumor vasculature,¹⁷ and accumulate within the tumor due to the enhanced permeability and retention (EPR) effect.¹⁹⁻²¹ Conjugating antibodies to nanoparticles has been shown to increase their therapeutic effect.²² Thus, conjugating anti-CD47 to nanoparticles may increase the effectiveness of anti-CD47 antibody in inducing phagocytosis *in vivo* by delivering the antibody selectively to the tumor.

In this study, we investigate the conjugation of anti-CD47 antibody to gold nanoparticles via click chemistry. Gold nanoparticles were synthesized¹ and conjugated to anti-CD47 antibodies.² Successful conjugation was confirmed using an ELISA assay and the cytotoxicity of the anti-CD47-gold nanoparticle conjugated product on cells was assessed *in vitro* with a cell viability assay. Future work will assess the conjugated antibody-nanoparticle's therapeutic effect

on cancer cells in the presence of macrophages, measured by its ability to induce phagocytosis of the cancer cells.¹³

1.1 Cancer By The Numbers

Cancer is the group of diseases characterized by uncontrolled cell growth leading to the proliferation of abnormal cells.²³ It is currently the second leading cause of death in the world.²³ According to an American Cancer Society study, 7.6 million people worldwide died from cancer in 2008, and that number is expected to grow to 13.2 million annual deaths by 2030, which is over 36,000 lives everyday.²³

Cancer's enormous impact on society has made it one of the most highly funded topics of research in the world.^{24,25} The American Cancer Society is currently funding over \$462 million in grants for cancer research²⁴ and the federally funded National Cancer Institute has had an average annual budget of \$4.9 billion over the past six years.²⁵ The incredible amount of time, money, and resources that have been put into cancer research has resulted in new and more effective cancer therapy strategies that have raised the overall average 5-year cancer survival rate in the United States from 50% in 1976 to 68% in 2007.²⁶ While this increased survival rate has undoubtedly impacted many lives, there are still currently 21,000 cancer deaths worldwide every day,²³ showing the desperate need for continued research to improve the effectiveness of modern cancer therapy treatments.

1.2 History of Cancer Therapy Approaches

Surgical Removal of Primary Tumors

Surgically removing tumors is the oldest known form of cancer therapy.²⁷ According to inscriptions found in Egypt, surface tumors have been surgically removed in a similar manner to how they are today since 1500 BC.²⁷ With the advent of general anesthesia in 1846, the door was opened for the possibility of more advanced surgical procedures.

These treatments were at first very invasive, removing both the tumor and surrounding healthy tissue; such as the radical mastectomy approach developed in the 1880s of removing the entire breast and surrounding chest muscles to treat breast cancer.²⁷ Over the years, surgery techniques have become more refined, which has reduced recovery time and side effects after

surgery, but the primary tumor is typically not the cause of death. As many as 90% of cancer deaths are caused by the metastasis of cancer cells – the spread of the cancerous cells from the primary tumor to other parts of the body – rendering surgical removal of the primary tumor an ineffective treatment option on its own.²⁸

Chemotherapy

Given the dangers of metastasis and evidence that localized treatment approaches had plateaued at a 33% cure rate,²⁹ the 1960s ushered in an era of investigating chemical drugs for their therapeutic effects. Fighting cancer with chemical drugs was termed “chemotherapy” and the medical field of oncology was officially established in 1972.²⁹

Chemotherapy drugs typically target rapidly dividing cells and work by interfering with a these cell’s ability to divide and reproduce.²⁹ They are often used in combination therapy approaches consisting of either surgery to remove the primary tumor and then chemotherapy³⁰ or simultaneous administration of multiple types of chemotherapy drugs that work through different mechanisms.³¹ Such combination chemotherapy techniques have proven to be very effective at treating many types of cancer, such as metastatic testicular cancer, which has seen its cure rate improve from 10% in 1977 to 95% with modern day chemotherapies.²⁹ However, a major problem with these approaches is that the chemotherapy drugs are often not specific for cancer cells, as many healthy cells are rapidly dividing as well, resulting in a long list of adverse side effects including nausea, vomiting, hair loss, fevers, chills, weight loss, and peripheral edema.³² Moreover, the cytotoxic effect that chemotherapy drugs have on the body limits the maximum dosage that can be administered, putting an upper-limit on their maximum potential therapeutic effect.³¹

Targeted Therapy

The problems caused by the detrimental effects of chemotherapy drugs on healthy cells have led to the development of more targeted therapeutics. An increased understanding of the mechanisms underlying the proliferation of cancer cells has allowed for the development of a new class of drugs, which are highly selective for targets unique to cancer cells.³³ Their specificity increases the drugs effectiveness at treating the patient’s specific cancer while reducing harmful side effects by decreasing cytotoxicity to normal healthy cells.³³

In 2010, there were 22 FDA-approved targeted cancer therapies on the market.³⁴ These drugs work by modulating the activity of one or more proteins involved in cancer, such as inhibiting abnormal enzymes (Gleevec®),³⁵ blocking overexpressed growth signals (Iressa®),³⁶ or preventing the degradation of natural cancer fighting proteins (Velcade®).³⁷ Treating cancer by attacking specific pathways using targeted therapies such as these has been shown to be extremely effective at eliminating cancer cells with high specificity and is one of the most promising areas of cancer therapy research.³³

1.3 Current Monoclonal Antibody Therapies

Monoclonal antibodies are currently becoming one of the most common forms of targeted therapy with 12 FDA-approved monoclonal antibodies available as of 2010.³⁴ Monoclonal antibodies are an effective form of targeted therapy because of their specificity for binding to specific antigens as targets.³⁸ The structure of an antibody consists of a constant region specific for the organism from which the antibody is produced, and a variable region that bind highly selectively to a specific antigen (Figure 1).³⁹ Each antibody binds to a different antigen, and this high specificity for a given antigen target makes antibodies a useful tool for targeted therapy.

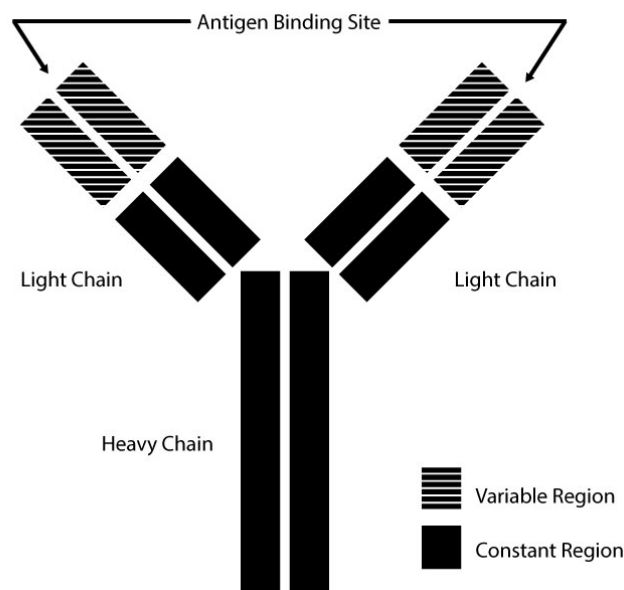


Figure 1. Antibody Structure: Variable and Constant Regions

A significant milestone for the use of antibodies therapeutically in humans was the development of humanized antibodies.³⁸ Originally the only way of studying the effects of an antibody treatment on cancer cells was to introduce an antigen into a mouse so that its immune system would produce antibodies that could be collected and studied specifically for that antigen. While using mice specific antibodies is useful for preliminary studies on the effect of the antibody in mouse models, the same antibody used in the mouse cannot be directly applied to

human trials because the constant regions of human and murine antibodies are significantly different and thus incompatible.³⁹ However, recently developed techniques can produce humanized antibodies from the mouse antibody by exchanging the murine constant region with a humanized constant region without altering the selectivity of the variable region.³⁸ This has greatly increased the speed of development and thus availability of humanized antibodies for cancer therapy.³⁸ All 12 FDA approved monoclonal therapies currently being used clinically are this type of humanized antibody.³⁸

1.4 CD47 as a Cancer Therapy Target

A newly discovered targeted monoclonal antibody therapy currently in Stage I clinical trials is anti-CD47.¹³ Recently, the transmembrane protein CD47 has been found to be an effective target for cancer therapies.¹³ This protein functions as an inhibitor of phagocytosis by ligating to SIRPα on macrophages, and serves as an anti-phagocytic signal.⁴⁰ CD47 is overexpressed on multiple types of cancer cells compared to healthy cells (3-fold more on average),¹³ including ovarian cancer, acute myeloid leukemia, chronic myeloid leukemia, acute lymphoblastic leukemia, non-Hodgkin's lymphoma, multiple myeloma, and bladder cancer.⁴⁰

Monoclonal anti-CD47 therapy has been demonstrated to be effective at inhibiting both primary tumor growth and tumor metastasis *in vitro* as well as in a mouse model (Figure 2).¹³ The results suggest that the blockade of CD47 with a monoclonal anti-CD47 antibody is potentially an extremely effective therapy for multiple types of cancer, and has received a \$20 million grant from the voter-funded California Institute for Regenerative Medicine to begin human trials of monoclonal anti-CD47 antibody.

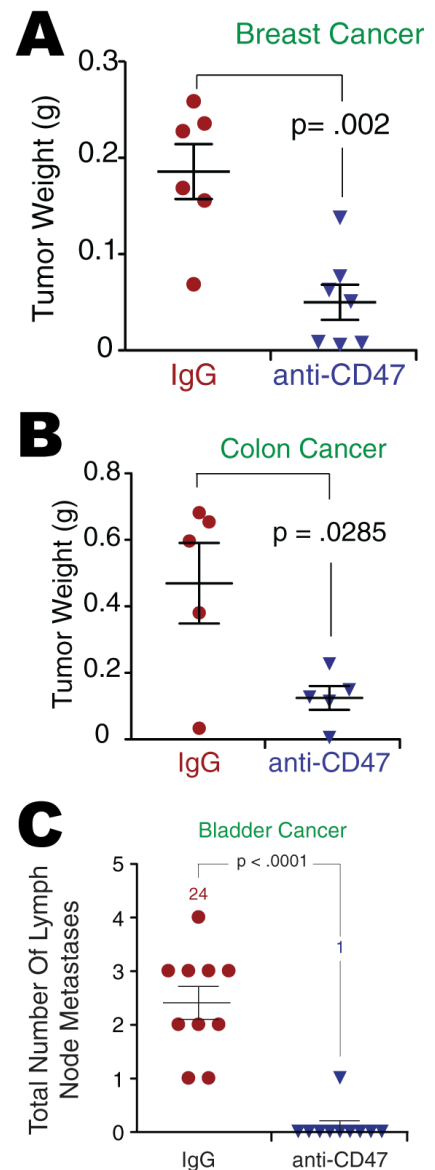


Figure 2. Anti-CD47 Therapeutic Effect. A&B, examples of inhibition of primary tumor growth. C, inhibition of tumor metastasis. From Weismann et al.¹³

It is hypothesized that anti-CD47 works through four different mechanisms.¹³ Its primary mechanism of action is the specific blockade of CD47, inhibiting the cell's anti-phagocytic signal through interaction with the SIRPα of macrophages, which enables phagocytosis of cancerous cells.¹³ Moreover, anti-CD47 monoclonal antibody treatment can also induce cancer cell death through the more traditional antibody therapy mechanisms such as natural killer-cell mediated ADCC and CDC,⁴¹ stimulation of apoptosis by a caspase-independent mechanism,⁴¹ as well as stimulation of an anti-tumor adaptive immune response.^{13,41}

A potential problem with this therapy, however, is that all normal cells in the body also express CD47, making anti-CD47 an untargeted and nonspecific therapy.¹³ Interestingly, despite CD47 being found on healthy cells, anti-CD47 does not show evidence of significant side effects *in vivo* besides temporary anemia.¹³ This is hypothesized to be caused by the fact that anti-CD47 antibody only blocks the negative phagocytic signal, and an additional positive phagocytic stimulus found only on cancer cells is also required for the cell to undergo phagocytosis (Figure 3).¹³ Therefore, although anti-CD47 binds to noncancerous cells, these healthy cells do not express any pro-phagocytic signal, causing them not to be engulfed by macrophages.

Despite the limited side effects observed in the mouse model there are additional potential side effects that are always concerns when administering antibody therapies, especially with high dose therapies.⁴² These side effects include hypersensitivity reactions, infusion reactions and immunogenicity, anemia, immunosuppression and infections, severe hypertension, and cardiovascular side effects including heart failure.⁴² As the anti-CD47 antibody treatment was found to be much more effective at higher doses,¹³ it would be extremely beneficial to be able to limit negative side effects by selectively delivering the antibody to the tumor in order to allow for a higher effective dose of anti-CD47 to be given clinically.

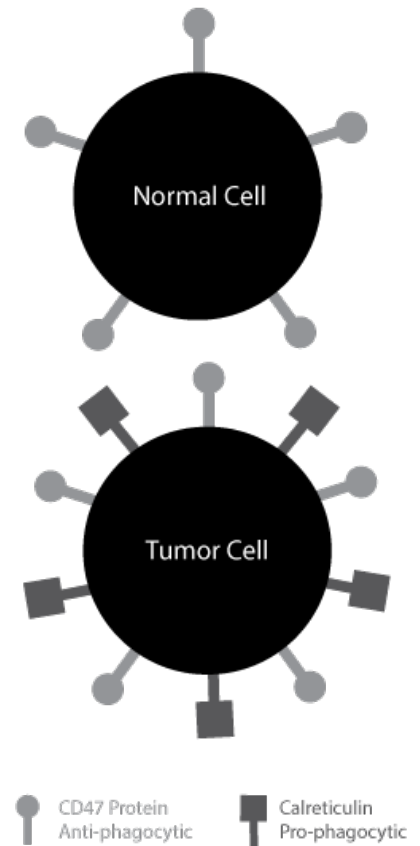


Figure 3. Normal and Cancerous cell comparison. Tumor cells express pro-phagocytic signals.

1.5 Nanoparticles as Directed Drug Delivery Systems

Mechanism of Drug Delivery Systems

Given the need to increase effectiveness while reducing side effects of this antibody therapeutic treatment, one possible solution is to use nanoparticles as a drug delivery system.¹⁵⁻¹⁷ Controlled drug delivery systems (DDS) transport the drug to the place of action in the body.¹⁷ This selectivity of delivery to the tumor effectively increases the drug's efficiency, reduces side effects, and decreases the dose required to achieve the desired effect.¹⁷ Nanoparticles, defined as being <100 nm in at least one dimension, are often used in DDS because of their unique ability to be effectively synthesized in a size controlled manner, to have large surface area to which multiple chemical moieties can be attached as ligands, and to exhibit natural aggregation in tumors.¹⁷

Nanoparticles are able to naturally aggregate in tumor cells because tumors have a hyper permeable vasculature.¹⁶ Due to the rapid cell proliferation and high mutation rate associated with tumor growth, the vasculature of the blood vessels near tumors becomes hyperpermeable ("leaky") to all molecules in the blood that are small enough to fit through its pores.^{43,44} Studies suggest that the cutoff size of the pores in this leaky tumor vasculature is very heterogeneous, but typically between 100 and 400 nm.^{16,45}

The leaky vasculature allows nanoparticles to accumulate in tumors because of the enhanced permeability and retention (EPR) effect (Figure 4).¹⁹⁻²¹ Nanoparticles are too large to fit through the pores of healthy tissue, allowing them to have circulation times in the blood upwards of 72 h.⁴⁶ This increased circulation time causes a large percentage of the nanoparticles to eventually find their way through the large leaky pores and into the tumor.¹⁹

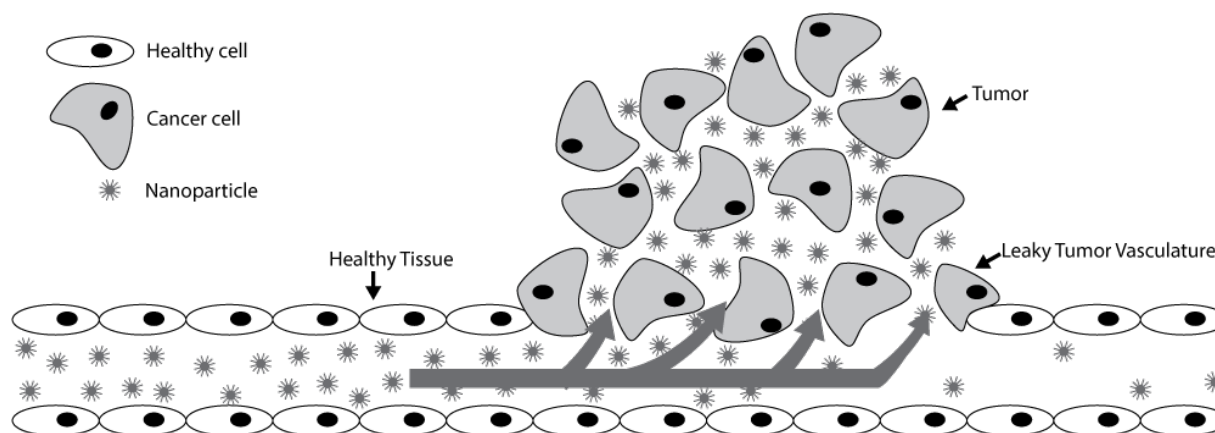


Figure 4. Leaky tumor vasculature allows for accumulation of nanoparticles due to EPR. Adapted from Brigger, et al.⁴⁵

While small enough to fit through the outermost pores, nanoparticles are also large enough to experience an increased retention rate once inside the tumor because they become lodged in areas of high cell density and small pore size, inhibiting their ability to diffuse out of the tumor site as easily as smaller molecules.^{19,20} Tumors also display characteristically diminished lymphatic drainage of large molecules, further increasing the retention rate of nanoparticles.¹⁹ Therefore, when injected intravenously, nanoparticles have been shown to exhibit increased accumulation in tumors because of their EPR effect.¹⁹⁻²¹

Benefit of Gold Nanoparticles

Gold nanoparticles are one class of nanoparticle that exhibit high accumulation in tumors because of the EPR effect.¹⁸ Gold particles are particularly advantageous to use for DDS because they are relatively easy to synthesize and functionalize, as well as highly biocompatible.¹⁸ Gold nanoparticles can be synthesized to be as small as 2 nm in diameter.¹⁸ When synthesized this small, the nanoparticles are hyperpermeable to the tumor's leaky vasculature, and are better able to avoid detection by the immune system, leading to a longer circulation time.¹⁸ However, smaller sized nanoparticles also experience decreased retention rate inside the tumor as they are able to pass in and out of the tumor more easily than larger nanoparticles.¹⁹ Therefore, determining the ideal size for the gold nanoparticle is a balancing act of making them small enough to permeate the tumor and avoid detection by macrophages, but large enough to experience increased retention rate once inside.¹⁹⁻²¹

Different size gold nanoparticles have been shown to be effective tools for tumor detection,⁴⁷ controlled delivery and release of a conjugated drug,¹⁸ and gene delivery to cancer cells.¹⁵ For this study, the most important application is gold nanoparticle's ability to deliver a monoclonal antibody selectively to tumor cells.

Conjugation Methods

In addition to the size of the nanoparticles, an important consideration in an antibody-nanoparticle conjugated system is the conjugation method used to attach the two components.⁴⁸ The traditional method for conducting this conjugation has been the EDC coupling method, which forms amide bonds between the antibody and the nanoparticle's carboxylated thiols (Figure 5).⁴⁸ However, this reaction is not ideal because it is highly inefficient - typically only

conjugating 20% of the antibodies to a nanoparticle - making it a wasteful and expensive procedure.⁴⁸

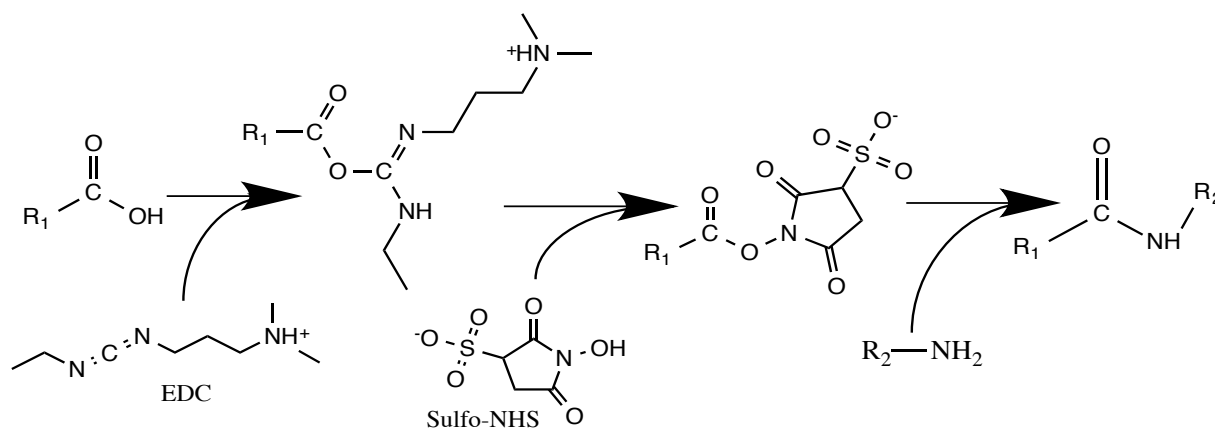


Figure 5. EDC coupled reaction. For our application the ligands would be: R_1 - Gold Nanoparticle; R_2 - Antibody

A new conjugation method utilizing “click chemistry” has been shown to produce a nearly 100% conjugation efficiency.⁴⁸ Click chemistry is the cycloaddition of an alkyne with an azide group in the presence of copper catalyst to form a 1,4-disubstituted-1,2,3-triazole (Figure 6).⁴⁹ This reaction is very promising for antibody-nanoparticle conjugation, as the alkyne and azide groups can be attached to the antibody and nanoparticle respectively, and then very efficiently “clicked” together to form a strong, stable covalent linkage.⁴⁹ Click chemistry has been shown to conjugate more than twice as many antibodies per nanoparticle than EDC coupling.⁴⁸

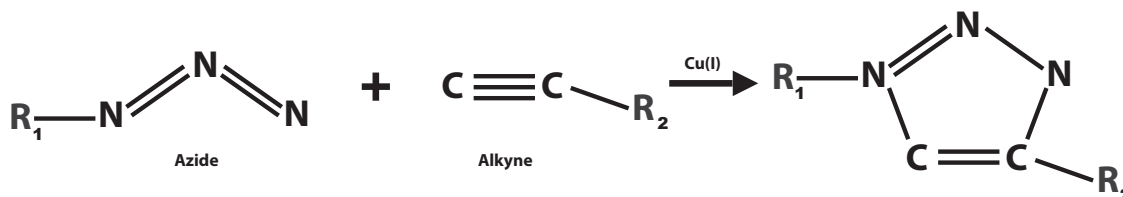


Figure 6. Click Chemistry Reaction. For our application the ligands are: R_1 - Gold Nanoparticle; R_2 - Antibody

1.6 Anti-CD47 Conjugated Gold Nanoparticle Therapy

In this study, we will investigate the conjugation of anti-CD47 monoclonal antibody to gold nanoparticles via click chemistry for cancer therapy. The procedure involves the synthesis of gold nanoparticles, followed by its conjugation to anti-CD47 antibody via click chemistry to produce a conjugated antibody-nanoparticle product (Figure 7). A successful conjugation will be assessed by an ELISA assay, and the final product's cytotoxicity to cells will be investigated by an *in vitro* cell viability assay. If the conjugation is successful and the product displays no significant cytotoxicity to cells on its own then it can be considered a viable option to be assessed for its therapeutic effect.

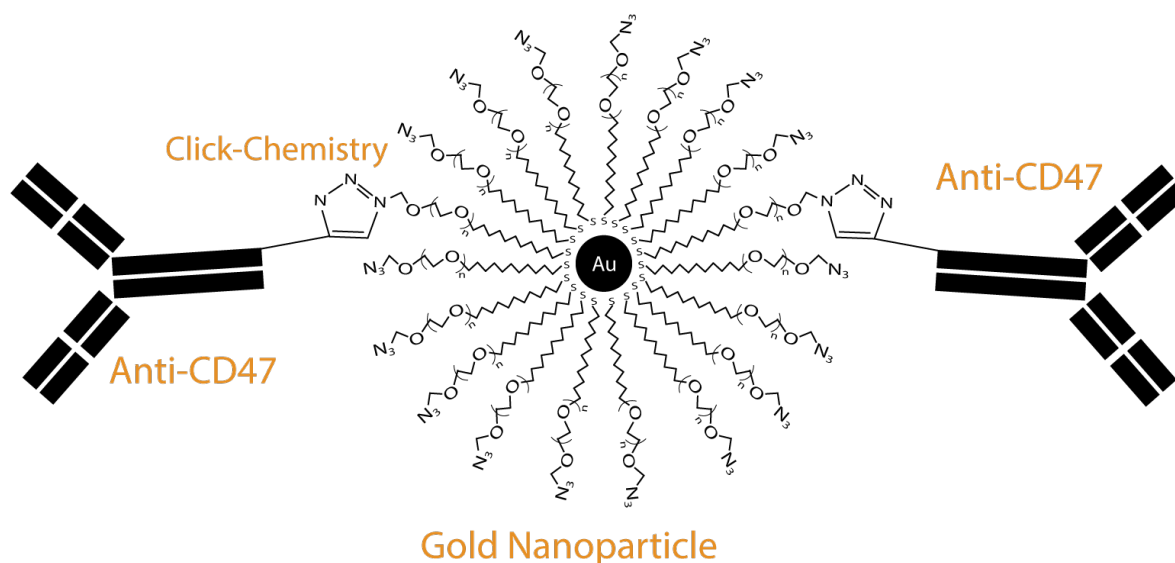


Figure 7. Anti-CD47 Conjugated Gold Nanoparticle Cancer Therapy Drug. Antibody ~15 nm, Au-NP ~30 nm

2. Materials and Methods

2.1 Materials

All chemicals used in this study were of analytical grade and were used as received from the suppliers without any further purification unless otherwise noted. Tetrachloroauric(III) acid trihydrate (Acros Organics); Tetraoctylammonium bromide (Sigma-Aldrich); 1-Dodecanethiol (Sigma-Aldrich); Sodium borohydride (Sigma-Aldrich); 11-Bromo-1-undecanethiol (Sigma-Aldrich); Sodium azide (Sigma-Aldrich); CRL-5928 *Homo sapiens* lung carcinoma cells (ATCC); RPMI-1640 Medium (ATCC); Anti-CD47 antibody [B6H12.2] (Abcam); Azido PEG thiol (Nanocs); Amicon Ultra-0.5 ml, Ultracel-100 Membrane centrifugal filter, 100 kDa (Millipore); Propargyl-dPEG₁-NHS ester (Quanta Biodesign); Zeba Spin Desalting columns, 7K MWCO, 0.5 ml (Thermo Scientific); Copper (III) sulfate pentahydrate (Sigma-Aldrich); L-Ascorbic acid (Sigma-Aldrich); Express ELISA Kit, Mouse (Genscript); Recombinant Human CD47 (Novoprotein); Cell counting kit-8 (Dojindo)

2.2 Dodecanethiolate Gold Nanoparticle Synthesis¹

Dodecanethiolate-gold nanoparticles (3 nm) were synthesized using the Schiffrin-Brust method.¹ An aqueous solution of hydrogen tetrachloroaurate (150 ml, 16.7 mM) was vigorously mixed with a solution of tetraoctylammonium bromide in toluene (150 ml, 26.7 mM) for 15 min at room temperature. Dodecanethiol (3.05 mmol) was stirred into the mixture for 5 min. An aqueous solution of sodium borohydride (10 ml, 5 M) was added dropwise under vigorous stirring and the reaction was subsequently stirred at room temperature for 3 h. The organic phase was collected and excess toluene was removed using a rotary evaporator. The nanoparticles were resuspended in minimal toluene, added to 500 ml of ethanol and kept in the dark at -20 °C for 72 h. The dark purple precipitate was collected by centrifugation and washed twice with ethanol before being redispersed in dichloromethane. The nanoparticles were characterized by ¹H NMR spectroscopy in CDCl₃ using a Bruker 400 Ultrashield spectrometer and found to be in agreement with the literature.² The size of the nanoparticles was measured with dynamic light scattering using a Zetasizer Nano ZS (Malvern Instruments) in chloroform at UMass Medical School (Han Lab, Biochemistry and Molecular Pharmacology Department).

2.3 Ligand Exchange with Bromoundecanthiol²

A thiol-ligand exchange of bromoundecanthiol was performed on the dodecanethiolate-gold nanoparticles to prepare the particles for the subsequent azide ligand exchange.² A solution of dodecanethiolate-gold nanoparticles in dichloromethane (200 ml, 0.715 mg/ml) was mixed with 500 mg of bromoundecanthiol under N₂ at room temperature for 5 days. The solvent was evaporated and the gold nanoparticles were washed with acetone and ethanol by centrifugation to remove excess thiol before resuspension in dichloromethane.

2.4 Azidation of Gold Nanoparticles²

Azide was substituted for bromide on the bromoundecanthiol-nanoparticles in preparation for the click chemistry reaction.² A solution of bromoundecanthiol-gold nanoparticles (12 ml, 9.17 mg/ml) dissolved in dichloromethane was mixed with an equal volume solution of sodium azide in dimethyl sulfoxide (DMSO) (0.235 M). The mixture was stirred for 48 h under N₂ at room temperature. An equal volume (24 ml) of deionized water was added before collecting the dark purple organic phase using a separatory funnel. The organic extract was dried over sodium sulfate and washed with ethanol before being collected by centrifugation and resuspended in dichloromethane. The azide-functionalized gold nanoparticles were characterized by ¹H NMR spectroscopy in CDCl₃ using a Bruker 400 Ultrashield spectrometer and found to be in agreement with the literature.² The size of the nanoparticles was measured with dynamic light scattering using a Zetasizer Nano ZS (Malvern Instruments) in chloroform at UMass Medical School (Han Lab, Biochemistry and Molecular Pharmacology Department).

2.5 Cell Culture Method

Homo sapiens lung carcinoma cells (NCI-H2170) were grown in culture according to the ATCC protocol. Upon arrival the entire vial of cells was thawed, mixed with 10 ml of RPMI-1640 (10% FBS) medium, and seeded on a 100 mm x 20 mm treated polystyrene cell culture dish. The cells were incubated at 37 °C in a 5% CO₂ air atmosphere. The medium was replaced every 24 h until the cells reached ~70% confluence (4 days). The cells were subsequently split 1:2 for the duration of the investigation whenever they reached 80% confluence (every 2-3 days).

2.6 Cytotoxicity of Dodecanethiolate and Azidoundecanethiolate Nanoparticles

The cytotoxicities of the synthesized dodecanethiolate and azide-functionalized nanoparticles were measured with a cell counting kit-8 (CKK-8) according to the manufacturer's protocol (Dojindo). *Homo sapiens* lung carcinoma cells were seeded on a 96-well plate in RPMI-1640 medium (10% FBS) at a density of 25,000 cells/well. The dodecanethiolate nanoparticles were collected by taking a 1 ml sample from the prepared stock solution and evaporating the dichloromethane using a rotary evaporator. Although the nanoparticles were not water-soluble and therefore could not be fully redispersed in water, they were mixed vigorously with deionized water until most of the nanoparticles had formed into small clumps floating in solution that could be pipetted. The same approach was implemented to collect a sample of the azide-functionalized gold nanoparticles in water.

Qualitative amounts of both types of gold nanoparticles were added to cell wells in triplicate after the initial 24 h incubation (Table 1). After incubation at 37 °C for an additional 24 h, the medium was removed and the cells were washed once with 1X phosphate-buffered saline (PBS). Fresh medium (90 μ l /well) and CKK-8 solution (10 μ l /well) were added and incubated at 37 °C for 4 h. Absorbance (450 nm) was subsequently measured using a Bio-Tek Synergy HT multi-mode microplate reader as a measure of cell viability. The solution containing CKK-8 was discarded and 100 μ l of fresh medium was added to each well. The plate was incubated at 37 °C for an additional 24 h before repeating the assay to measure cell viability at 48 h. The mean viability of each test group (\pm S.E.) was graphed using Microsoft Excel.

Table 1. Plate layout of cytotoxicity assay of gold nanoparticles.

Condition	Medium (μ l)	Gold Nanoparticles (μ l)
Control	100	0
Dodecanethiol AuNP	90	10
Azide-functionalized AuNP	90	10

*Each condition repeated in triplicate. (n=1)

2.7 Azido-PEG-Thiol Gold Nanoparticle Modification^{50,51}

The dodecanethiolate gold nanoparticles were modified with a thiol-PEG-azide compound to make azide-attached gold nanoparticles that are water-soluble.^{50,51} Dodecanethiolate gold nanoparticles were collected from the previously prepared stock solution using a rotary evaporator and redispersed in dichloromethane (2 ml, 1.8 mg/ml). Azido-PEG-thiol (3k Da) was dissolved in dichloromethane (2 ml, 30 mg/ml) and mixed with the nanoparticles overnight under N₂ at room temperature. The now water-soluble nanoparticles were washed twice with deionized water and redispersed in deionized water.

2.8 Anti-CD47 Antibody Functionalization^{50,51}

Anti-CD47 monoclonal antibody (B6H12.2) was functionalized for the click chemistry reaction by the addition of an alkyne group.^{50,51} The solution that the antibody was shipped in contained 0.09% sodium azide, which needed to be removed so that it would not react with the alkyne compound. Anti-CD47 solution (250 μ l) was added to a size exclusion centrifugal filter (100K MWCO) and centrifuged at 14,000 rcf for 10 min. The flow-through was discarded, and the filter was flipped upside down in a clean Eppendorf tube and centrifuged at 1,000 rcf for 2 min. An additional 50 μ l 1X PBS was added to the extracted solution. A solution of propargyl-PEG-NHS ester (2 μ l, 100 mg/ml dissolved in DMSO) was added to this antibody solution, and the reaction was kept in 4 °C for 6 h.

The functionalized antibodies were then purified from unreacted alkyne by applying the reaction solution to the resin bed of a desalting column (7K MWCO) and centrifuging at 1,500 rcf for 2 min. An additional 50 μ l 1X PBS was added to the flow through to fully resuspend the antibodies.

2.9 Conjugation of Anti-CD47 to Gold Nanoparticles via Click-Chemistry^{50,51}

The alkyne-functionalized anti-CD47 antibodies were conjugated to the azide-PEG-gold nanoparticles via click chemistry.^{50,51} Alkyne-functionalized antibody in solution (200 μ l, 0.25 mg/ml dissolved in 1X PBS) was mixed with a 30 μ l azide-PEG-AuNP solution (1 mg/ml dissolved in deionized H₂O). Copper sulfate (20 nmol) was added to the reaction as a catalyst, followed by the dropwise addition of ascorbic acid (100 nmol). The reaction was incubated at 4

°C for 24 h. The solution was subsequently centrifuged at 10,000 rcf for 10 min. At this speed any antibody that precipitated out of solution must be conjugated to gold nanoparticles, and any unreacted antibody would stay in solution. The resulting pellet was resuspended in deionized water and the efficacy of the conjugation was assessed by an ELISA assay.

2.10 ELISA Assay

An ELISA assay was conducted (according to the manufacturer's protocol, Genscript) to test for the presence of anti-CD47 antibody. The click chemistry reaction solution was tested after it was centrifuged at a speed (10,000 rcf) so that any antibody present must be conjugated to gold nanoparticles. A solution of 400 μ l recombinant human CD47 (20 μ g/ml in deionized H₂O) was diluted to 10 μ g/ml with 2X coating buffer. This diluted antigen solution was added to each well (100 μ l /well) and incubated at room temperature for 5 min. The solution was removed and the wells were treated with an equal part solution of pretreat A and pretreat B (200 μ l /well). After 5 min of incubating at room temperature, the wells were washed three times with 1X wash solution (250 μ l /well). The test solutions were subsequently added to each well (Table 2), and brought to a final volume of 100 μ l with 1X PBS.

Table 2. Plate layout of anti-CD47 ELISA assay.

Condition	Test Solution (μ l)	1X PBS (μ l)
Control	0	100
Stock anti-CD47 antibody	50	50
Alkyne-conjugated anti-CD47	20	80
Anti-CD47-AuNP final product	100	0

*Each condition repeated in triplicate. (n=1)

The plate was incubated at room temperature for 30 min before being washed once with 1X wash solution (200 μ l /well). ELISA solution was added (100 μ l /well) and incubated at room temperature for 20 min. The wells were thoroughly washed 5 times with 1X wash solution (200 μ l /well). One-solution Microwell TMB substrate solution was added (100 μ l /well) and allowed to incubate for 15 min at room temperature with gentle shaking. The reaction was stopped with the addition of Stop solution (100 μ l /well), and absorbance at 450 nm was immediately

measured using a Bio-Tek Synergy HT multi-mode microplate reader. The results were plotted using Microsoft Excel and significance was assessed using a two-tailed T-test ($p < 0.1$).

2.11 Anti-CD47-AuNP Cytotoxicity Assay

The toxicity of the final antibody-nanoparticle conjugated product on cells was assessed using a cell-counting kit 8 (CCK-8) following the manufacture's protocol (Dojindo). *Homo sapiens* lung carcinoma cells were seeded on a 96-well plate in RPMI-1640 (10% FBS) medium at a density of 25,000 cells/well and incubated at 37 °C for 24 h. Test solutions were added to the cells in triplicate (Table 3). After incubation at 37 °C for an additional 24 h, the cells were washed once with 1X PBS. Fresh medium was added (90 μ l /well) as well as CCK-8 solution (10 μ l /well). The plate was incubated at 37 °C for 4 h. Absorbance (450 nm) was subsequently measured using a Bio-Tek Synergy HT multi-mode microplate reader as a measure of cell viability. The solution containing CCK-8 was discarded and 100 μ l of fresh medium was added to each well. The plate was incubated at 37 °C for an additional 48 h before repeating the assay to measure cell viability after 72 h. The mean viability of each test group (\pm S.E.) was graphed using Microsoft Excel.

Table 3. Plate layout of cytotoxicity assay of anti-CD47-AuNP final product.

Condition	Medium (μl)	Gold Nanoparticles (μl)
Control	100	0
Azide-PEG-AuNP	90	10
Anti-CD47-AuNP	90	10

*Each condition repeated in triplicate. (n=1)

3. Results and Discussion

In this study we investigated the conjugation of anti-CD47 antibodies to gold nanoparticles via click chemistry. The synthesis and azido-modification of the gold nanoparticles was confirmed by ^1H NMR spectroscopy, and their final size measured using dynamic light scattering. The efficacy of the click chemistry conjugation was assessed using an ELISA assay and fails to show evidence of a successful conjugation ($p > 0.05$). A cytotoxicity assay demonstrates no toxic effect of the click chemistry final product on cells *in vitro*, suggesting that the anti-CD47-gold nanoparticle conjugated product is a potentially viable candidate to be tested for its therapeutic effect as a cancer therapy agent.

3.1 Dodecanethiolate-Gold Nanoparticle Synthesis¹

Gold nanoparticles were synthesized using the Schiffrin-Brust method.¹ This method was followed because it is the approach I learned from Dr. Han (UMass Medical School) while working in his lab during the summer 2013. He used it throughout his Ph.D. studies of gold nanoparticles because of its simplicity and reliability in producing size controlled gold nanoparticles. I had performed the protocol successfully at UMass over the summer, but still conducted a preliminary “small batch” test run at Middlebury to double-check the efficacy of the synthesis protocol and make sure all the instruments at Middlebury were sufficient so as to not waste any of the expensive materials. The test run was conducted without any obvious problems and produced a final solution that visually looked identical to the product I made at UMass under Dr. Han’s guidance. I therefore proceeded to repeat the protocol in much higher quantities.

The quantities used for the full-scale gold nanoparticle synthesis were chosen under the guidance of Dr. Han who drew from his personal Ph.D. experience to suggest a quantity that would yield an amount of gold nanoparticles that would be sufficient for the entirety of the thesis without going over budget. As gold nanoparticles have been shown to be stable for over 6 months at room temperature,⁵² rapid deterioration of the synthesized nanoparticles was not a concern. Therefore it was easier to synthesize one large batch of dodecanethiolate-gold nanoparticles to use for subsequent tests and modifications rather than continuously performing small batch synthesis whenever more gold nanoparticles were needed.

The synthesis of gold nanoparticles involves the reduction of a gold complex in solution causing the gold to aggregate in very small clumps that can be stabilized with thiol chains (Figure 8).¹ Alterations to the gold-to-thiol ratio, or changing the length of time or temperature of the reaction allow for tight control over the nanoparticle's overall size, geometry, and monodispersion.¹ Furthermore, the nanoparticles are highly stable under physiological conditions, which is crucial because if they aggregate then they lose the benefit of their small size and may no longer be able to pass through the tumor's leaky vasculature, rendering them ineffective.¹⁸

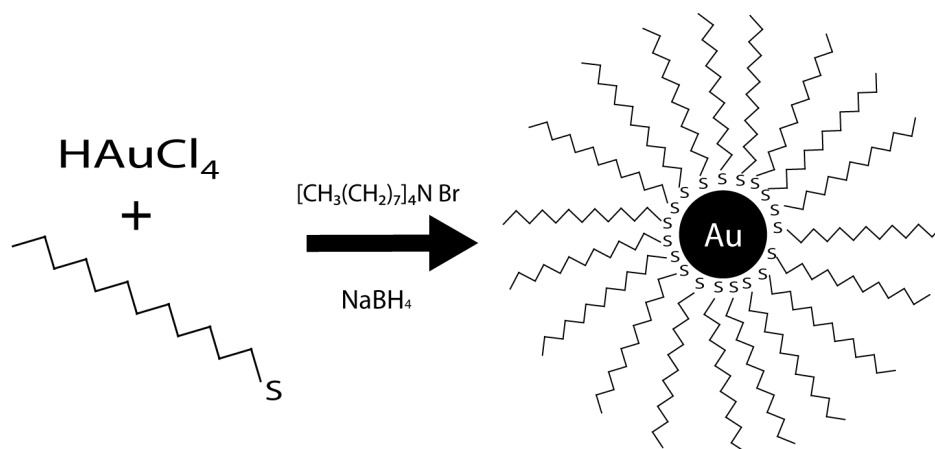


Figure 8. Synthesis of dodecanethiolate gold nanoparticles

Our synthesized nanoparticles were characterized by ¹H NMR spectroscopy and the spectrum was compared to known dodecanethiolate-gold nanoparticle ¹H NMR spectrum in the literature (Figure 9).² The spectra are almost identical, suggesting that the synthesis was successful. The size of the dodecanethiolate-gold nanoparticles was measured with dynamic light scattering (Zetasizer Nano Series, Nano ZS, Malvern Instruments) at UMass Medical School (Han Lab, Biochemistry and Molecular Pharmacology Department). Dynamic light scattering works by illuminating the sample solution with a laser, and the beam is scattered by the particles in solution. The intensity of the frequency shift of the scattered laser beam is measured over time, and can be used to calculate the hydrodynamic diameter of the particles based on Brownian motion of particles in solution.⁵³ The results show the nanoparticles are 2.8 ± 0.49 nm in diameter (Figure 10). This is almost exactly our expected size of 2 nm, and should make our final product after subsequent nanoparticle substitutions and antibody conjugations in the ideal size range of 10-100 nm for optimal natural accumulation in the tumor.¹⁹

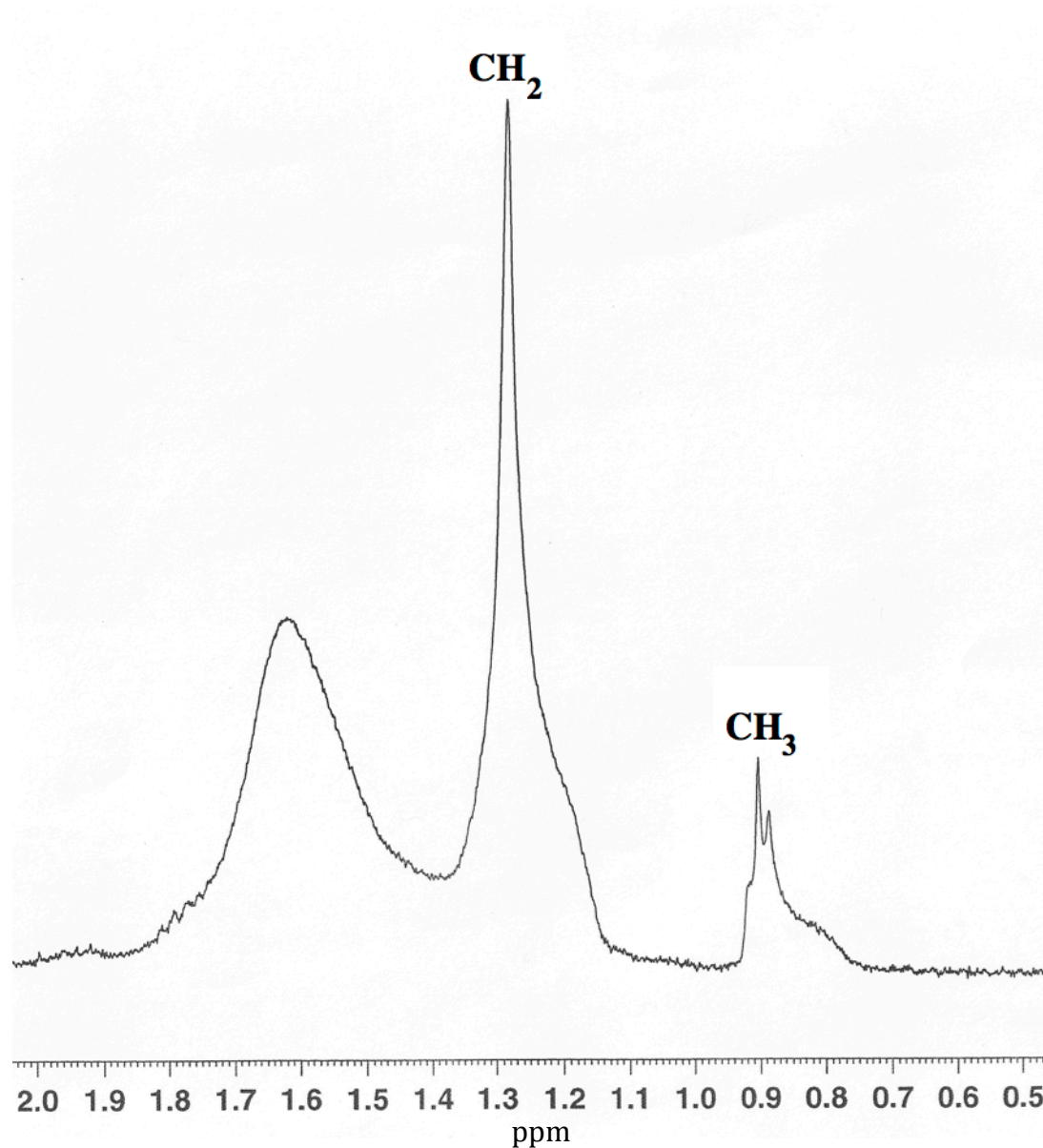


Figure 9. ^1H NMR spectrum of dodecanethiolate-AuNPs in CDCl_3 (δ ppm). ^1H NMR Bruker 400 Ultrashield spectrometer

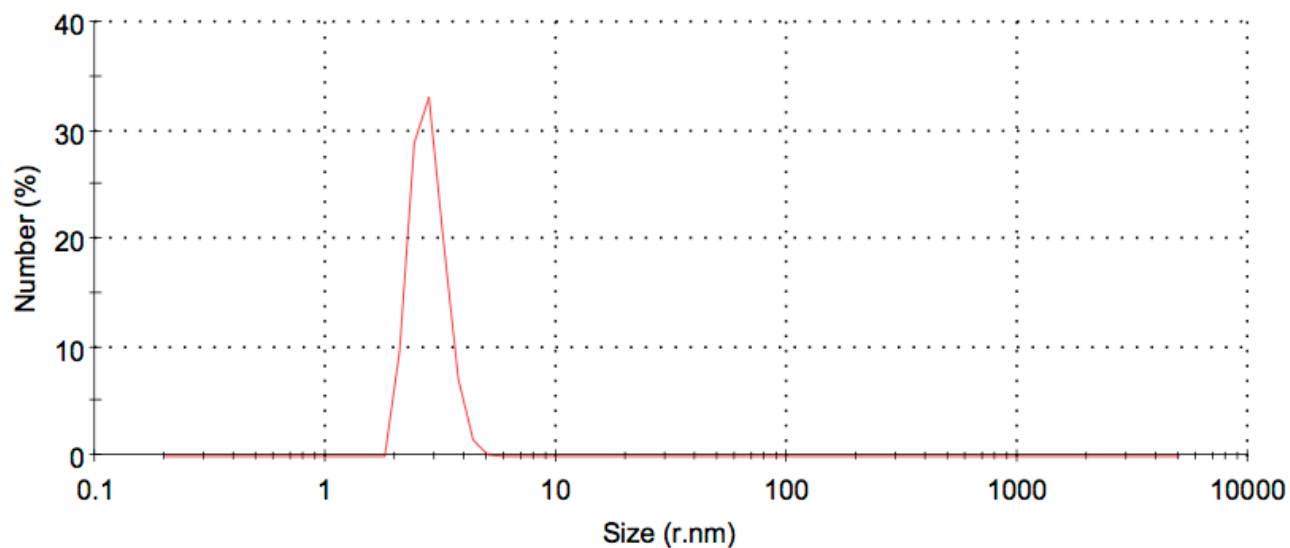


Figure 10. Size distribution of dodecanethiolate gold nanoparticles. Size peak 2.810 ± 0.49 nm. Measured with using a Zetasizer Nano ZS in chloroform at UMass Medical School (Han Lab, Biochemistry and Molecular Pharmacology Department).

3.2 Bromoundecanethiol and Azide Substitutions on Gold Nanoparticles²

A thiol-ligand exchange of bromoundecanethiol was performed on the dodecanethiolate-gold nanoparticles to prepare the particles for a subsequent azide substitution.² We decided to follow this method to prepare the nanoparticles for the click chemistry reaction because of its detailed step-by-step procedure found in the literature, as well as available ¹H NMR spectra with which to compare our results at each step.² A downside of this protocol is that it requires a large amount of bromoundecanethiol, which is very expensive (\$400 per 250 mg). Other approaches to attach the azide to the gold nanoparticles were considered in order to avoid this expensive compound, but were found to be much more complicated and had less detailed protocols in the literature. Therefore we decided to follow the higher cost method,² reasoning that its detailed protocol would not only be easier to follow, but also may in fact save money overall by avoiding wasteful failed experiments attempting to follow more vague protocols.

The thiol-ligand exchange of bromoundecanethiol appeared to proceed without any noticeable problems, such as visible nanoparticle aggregation. A 10-fold excess of 1-bromoundecanethiolate was mixed with our synthesized dodecanethiolate gold nanoparticles in dichloromethane (Figure 11). This method has been shown to produce gold nanoparticles in which an average of 75% of the undecanethiolate ligands are now bromoundecanethiol and 25% remain dodecanethiol.²

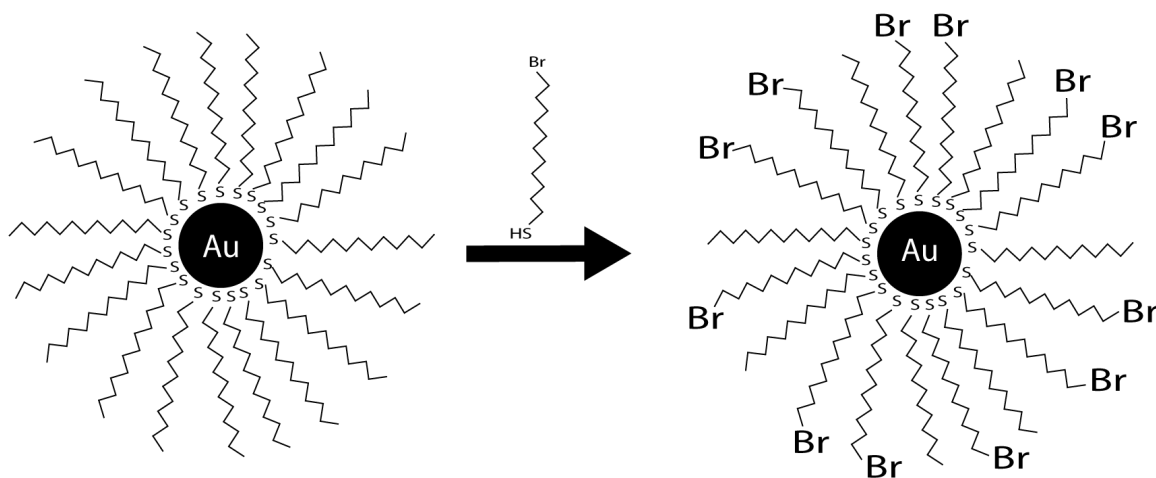


Figure 11. Thiol-ligand exchange of bromoundecanethiol on dodecanethiolate gold nanoparticles

Azide substitution was subsequently conducted in order to attach an azido group to the gold nanoparticles in preparation for the click chemistry reaction. A nucleophilic substitution of azide for bromide was achieved by reacting 20-fold excess NaN_3 with bromoundecanethiol gold nanoparticles (Figure 12). The resulting nanoparticles were characterized by ^1H NMR spectroscopy (Figure 13). The appearance of a peak at 3.41 ppm characteristic of the $\text{CH}_2\text{-N}_3$ protons is very close to the peak reported in the literature (3.26 ppm), suggesting our azide substitution was successful.

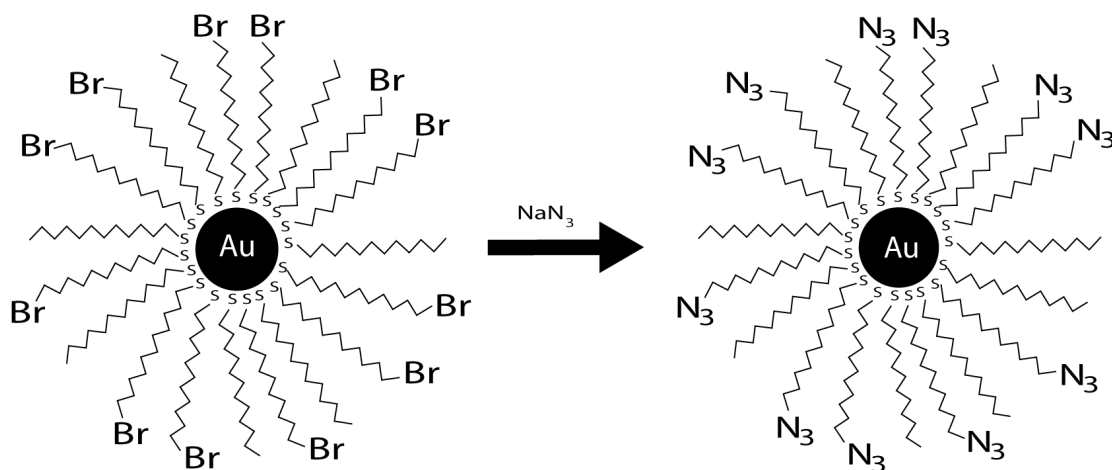


Figure 12. Azide substitution on bromoundecanethiol gold nanoparticles

The size of the azidoundecanethiolate-gold nanoparticles was then measured with dynamic light scattering (Zetasizer Nano Series, Nano ZS, Malvern Instruments) at UMass Medical School (Han Lab, Biochemistry and Molecular Pharmacology Department). The results show the modified nanoparticles to be 21.37 ± 3.28 nm in diameter (Figure 14). This is an unexpectedly large increase in size from the 2.8 nm dodecanethiolate gold nanoparticles due to the addition of the azido group alone. Such a large increase in size suggests that mild aggregation of the azidoundecanethiolate gold nanoparticles occurred. While any aggregation is not ideal, the fact that the slightly aggregated azido-gold nanoparticles are still only 21 nm suggests that our final conjugated antibody-nanoparticle product will still be in the ideal size range of 10-100 nm for natural accumulation in the tumor.¹⁹ Therefore, the azidoundecanethiolate appear to be in acceptable condition to proceed to the click chemistry reaction despite the mild amount of aggregation.

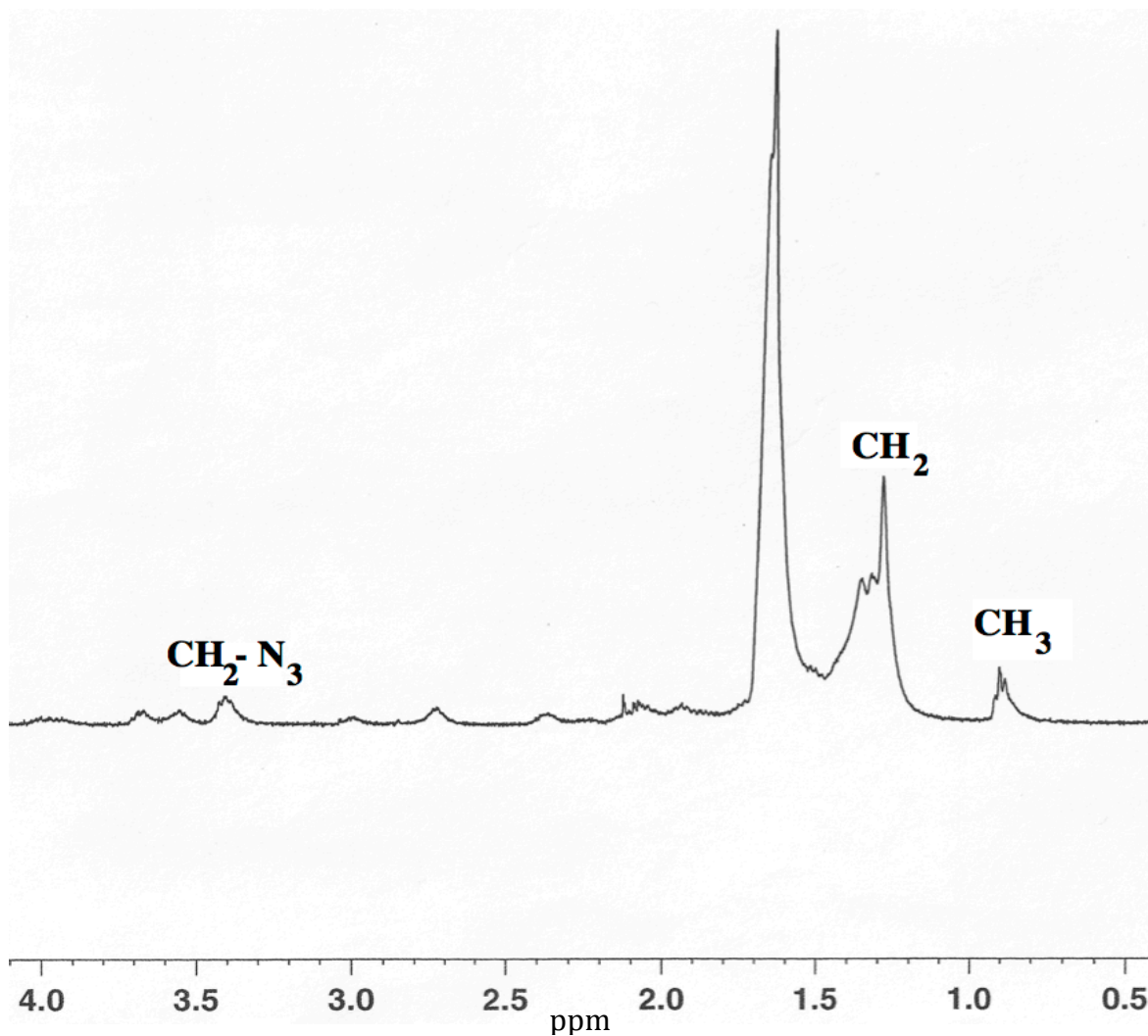


Figure 13. ^1H NMR spectrum of azideundecanethiolate-AuNPs in CDCl_3 (δ ppm). ^1H NMR Bruker 400 Ultrashield spectrometer

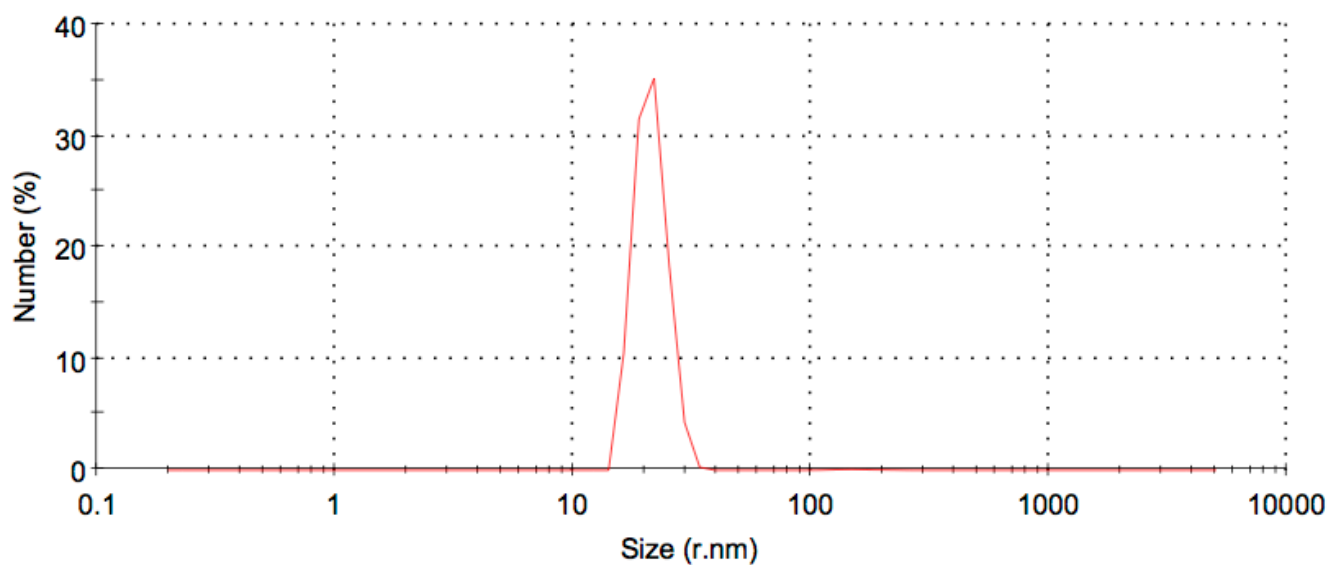


Figure 14. Size distribution of azideundecanethiolate gold nanoparticles. Size peak 21.37 ± 3.28 nm. Measured with using a Zetasizer Nano ZS in chloroform at UMass Medical School (Han Lab, Biochemistry and Molecular Pharmacology Department).

3.3 Cytotoxicity of Dodecanethiolate and Azidoundecanthiolate Gold Nanoparticles

The cytotoxicity of the nanoparticles on cells was assessed *in vitro* using a cell counting kit-8 (CCK-8). The CCK-8 test was chosen because it is fast, inexpensive, and doesn't have a toxic effect on the cells so it can be used to measure cell viability over multiple time points. In this assay, the cells are incubated with water-soluble tetrazolium salt for 4 h, in which the salt is reduced by dehydrogenase activity in any living cell to produce a yellow formazan dye product. The yellow dye changes the color of the solution so that absorbance (450 nm) of each well can subsequently be assessed as a measure of cell viability, since the absorbance of the well is directly proportional to the number of living cells.

The most difficult aspect of conducting the test was the cell culture aspect. *Homo sapiens* lung carcinoma cells (NCI-H2170) were used throughout the thesis in anticipation of possibly having time to conduct a phagocytosis assay with our final product to assess its ability to induce phagocytosis of cancer cells by macrophages. We wanted to have the necessary cancer cells ready in case we had enough time to perform such assay by the end of the year, and since the cytotoxicity assays can be conducted on any type of cell we used this opportunity to begin culturing a lung cancer cell line. This cell line was somewhat difficult to culture, as it requires a high minimum confluence in order to grow, but once reached grows to maximum confluence extremely quickly (60 h). It took a number of weeks and close calls of almost losing the cells due to the confluence of the cells being too high or too low before we were able to perfect the timing and ratio of how to split the cells. Furthermore, we experienced multiple incubator mechanical problems that caused long delays as they were being fixed. The entire month of January was spent growing and freezing back numerous vials of cells so that we would never run out of available cells regardless of what unexpected technical issues we experienced. This proved very useful in the spring, as we had to thaw vials of frozen cells multiple times after losing cells because of incubator complications and bacterial contamination.

The dodecanethiolate and azidoundecanethiolate gold nanoparticles showed no significant toxic effect on cells *in vitro* (Figure 15). The fact that there was no observed toxic effect suggests that these nanoparticles are a viable option to be used for the directed delivery of anti-CD47 antibody. The error bars are quite large for this experiment suggesting it would be ideally repeated in the future, the lack of toxicity is substantiated by numerous reports in the literature suggesting gold nanoparticles have low cytotoxicity both *in vitro* and *in vivo*.⁵⁴⁻⁵⁶

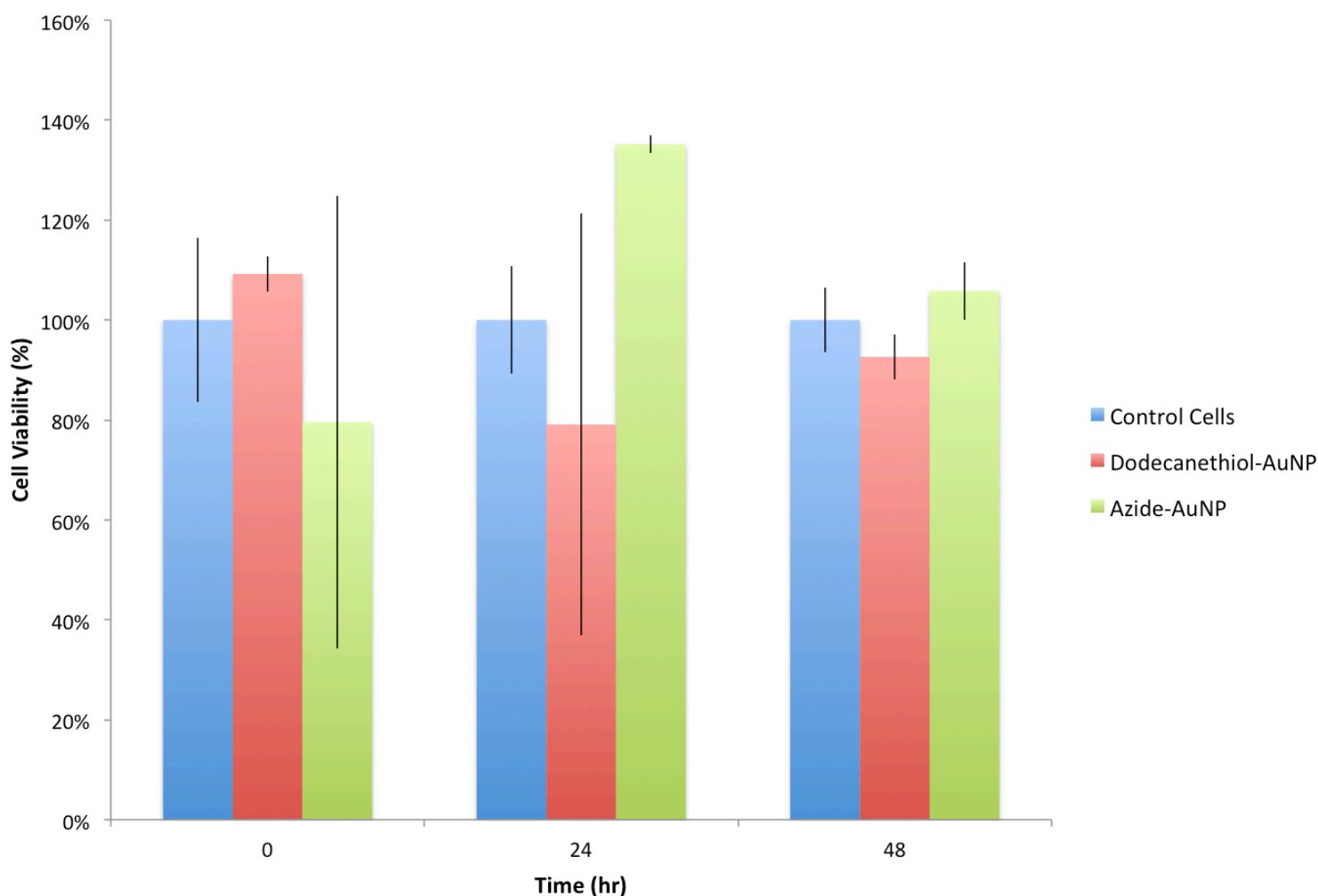


Figure 15. Cytotoxicity of dodecanethiolate and azidoundecanethiolate gold nanoparticles *in vitro*. Cell viability measured using cell counting kit-8 according to manufacturer's protocol (Dojindo). *Homo sapiens* lung carcinoma cells (NCI-H2170).

3.4 Thiol-PEG-Azide Nanoparticle Modification and Antibody Functionalization^{50,51}

While preparing the gold nanoparticles for the click chemistry reaction, we found that the azidoundecanethiolate gold nanoparticles were not water-soluble. The protocol we had followed to modify the nanoparticles with the azide group² conjugated compounds soluble in organic solvents to the gold nanoparticles and thus were not concerned with the nanoparticles water-solubility. Our goal, however, is to conjugate antibodies to the nanoparticles, which cannot be delivered in an organic solvent. Therefore, we went back to the literature to find an approach to make our azideundecanethiolate gold nanoparticles water-soluble. We found a new method that utilizes a thiol-ligand substitution of thiol-PEG-azide (Quanta Biodesign) with our synthesized dodecanethiolate gold nanoparticles to produce water soluble nanoparticles that contain an azide group (Figure 16).^{50,51} No NMR spectroscopy was needed to confirm a successful thiol-ligand substitution as the fact that the nanoparticles became water-soluble is sufficient to demonstrate that the exchange was successful.

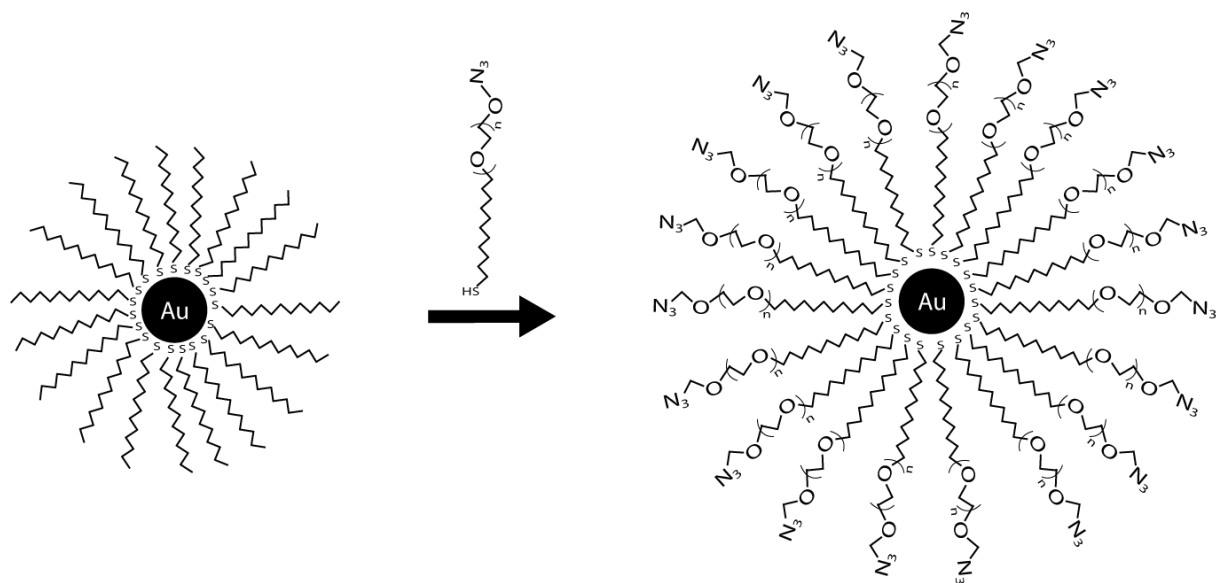


Figure 16. Thiol-PEG-Azide modification of gold nanoparticles for water solubility.

Anti-CD47 antibody was functionalized in preparation for the click chemistry reaction by the attachment of an alkyne following established methods in the literature.^{50,51} The propargyl-dPEG-NHS ester reacts with amines found in the structure of the antibody to attach the alkyne (Figure 17). A potential problem is that there are a number of amine groups as part of the

structure of an antibody (Figure 18) and this conjugation method does not allow for control over which amine the alkyne attaches.⁵⁷ Therefore, it is possible the alkyne could attach to part of the Fab region of the antibody in such a position that subsequent conjugation of a gold nanoparticle could place the nanoparticle in a position blocking the antigen-binding site, rendering the antibody ineffective in binding CD47 protein.

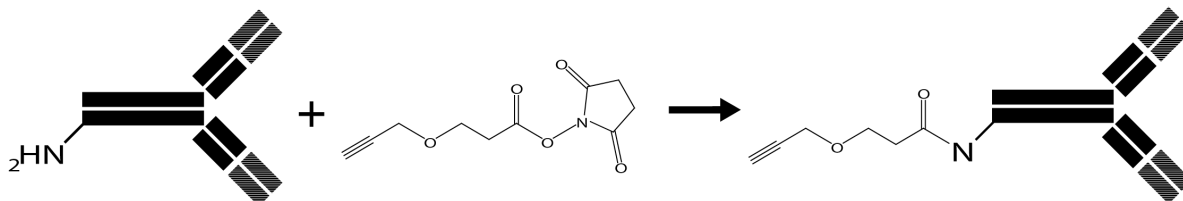


Figure 17. Functionalization of anti-CD47 antibody with propargyl-dPEG-NHS ester.

This is a consideration to take into account when accessing the therapeutic effect of the final anti-CD47-nanoparticle product in the future if it is found that our final product is less effective in binding CD47 than the antibody alone. If this is the case then new experimental methods for attaching the alkyne to the antibody could be utilized.⁵⁸ However, numerous studies have utilized the propargyl-dPEG-NHS ester in reaction with antibodies and have not reported any detrimental effects to the utility of the antibody.^{3,4}

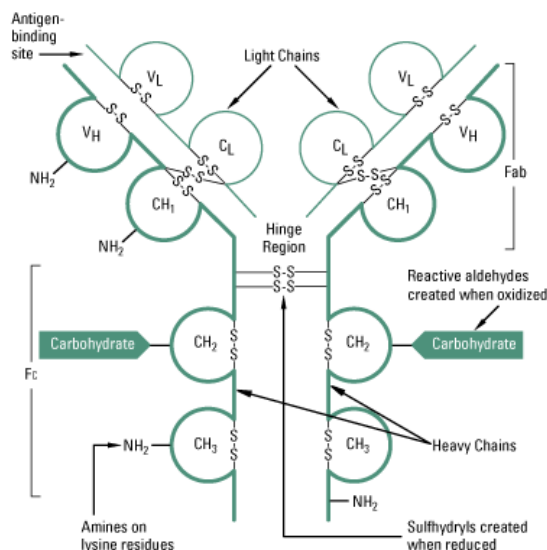


Figure 18. Amine groups part of antibody structure.⁵⁷ Propargyl-dPEG-NHS ester compound reacts with any amine group during antibody functionalization with alkyne for click chemistry.

3.5 Conjugation of anti-CD47 antibodies to gold nanoparticles via click chemistry²⁻⁴

Alkyne-functionalized anti-CD47 antibodies were conjugated to azidoundecanethiolate-gold nanoparticles via click chemistry.²⁻⁴ Click chemistry is the cycloaddition of an alkyne with an azide group in the presence of copper catalyst to form a 1,4-disubstituted-1,2,3-triazole.⁴⁹ This reaction is very useful for antibody-nanoparticle conjugation, as the alkyne and azide groups can be attached to the antibody and nanoparticle respectively, and then very efficiently “clicked” together to form a strong, stable covalent linkage (Figure 19).⁴⁹

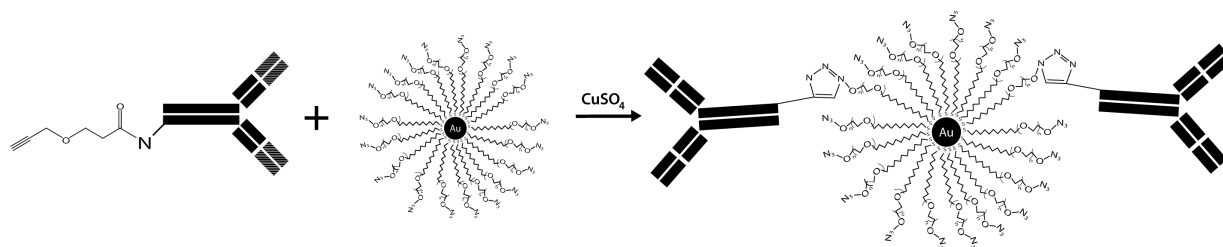


Figure 19. Click chemistry of alkyne-antibodies with azido-gold nanoparticles.

An ELISA assay was conducted to assess the efficacy of the conjugation. An ELISA assay detects the presence of antibodies by relying on the specificity of the antibody-antigen interaction between the desired antibody to be tested and its antigen immobilized to a solid surface. A secondary antibody linked to an enzyme is added so that it binds to any of the antigen-bound primary antibody present after washing away unattached primary antibody. The subsequent addition of a compound that produces a colored product when reacted with the enzyme can be used as a measure of how much primary antibody is present in solution. The more primary antibody present, then the more secondary antibody-bound enzyme remains in solution to produce the colored product. Thus, higher absorbance measurements indicate the presence of a larger quantity of the primary antibody. The results fail to suggest that the conjugation was successful, although there was an insignificant increase in absorbance of the wells treated with the click chemistry reaction solution over a negative control with no anti-CD47 present (Figure 20). A two-tailed T-Test found the increase in absorbance to be insignificant ($p > 0.05$).

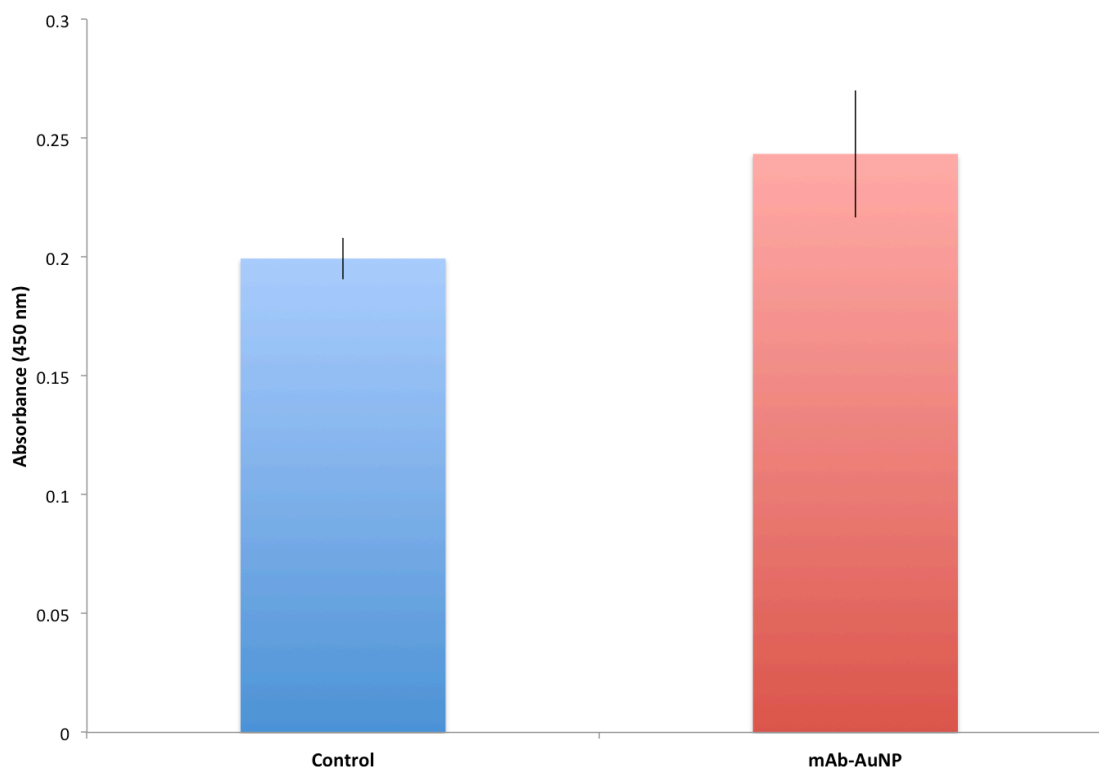


Figure 20. ELISA of click chemistry conjugation of anti-CD47 antibody to gold nanoparticles. Measured with Express ELISA kit (mouse) according to manufacturer's protocol. Recombinant human CD47 used as antigen. Anti-CD47-AuNP displays insignificantly higher absorbance than control of no antibody ($p < 0.05$) ($n=1$)

The insignificant increase in absorbance could be caused by (1) the low amount of final product produced or (2) the spatial conjugation of the nanoparticles on the antibody. Given budget constraints and the fact that we were developing this protocol for the first time, we made a very small amount of the final anti-CD47-nanoparticle conjugated product. The ELISA assay is a concentration dependent test, which measures the overall amount of anti-CD47 antibody in each well. Since we had so little of our final product, which was further spread over three wells to perform the test in triplicate, the only slight increase in absorbance could be due to the fact that there was a very small amount of final product in each test well. Another possible explanation could be due to the fact that the conjugation method does not allow us to control which part of the antibody the nanoparticles attach. It is possible that a number of nanoparticles attached to the Fc region of the antibodies, which would effectively block the binding of the secondary antibody during the ELISA test (Figure 18). Therefore, there may in fact be more successfully conjugated final product than is registering in the ELISA assay because the spatial location of the nanoparticles is blocking the secondary antibody from binding. If increasing the

amount of final product added to future ELISA assays does not produce a significant result, then other methods for testing for the presence of the antibody that would not be affected by the spatial location of the nanoparticles should be considered.⁵⁹

3.6 Cytotoxicity of Anti-CD47-AuNP Conjugated Final Product

The cytotoxicity of anti-CD47-AuNP on cells *in vitro* was assessed using a CCK-8 assay following the manufacturer's protocol (Dojindo). The anti-CD47-gold nanoparticles did not show any significant toxic effect on the cells (Figure 21). The fact that the anti-CD47-AuNP final product shows no toxicity to cells on its own suggests that it is a viable cancer therapy candidate and should be further tested for its therapeutic effect in inducing phagocytosis of cancer cells by macrophages. A surprising result of this CCK-8 assay is that the cells treated with thiol-PEG-azide gold nanoparticles showed much higher cell growth over the 72 h study than the control group (Figure 21). This would suggest that the PEG-nanoparticles promote cell proliferation, which is a very surprising result with no supporting evidence in the literature. Further work should be conducted to investigate if this result is an anomaly or a reproducible characteristic of thiol-PEG-azide gold nanoparticles.

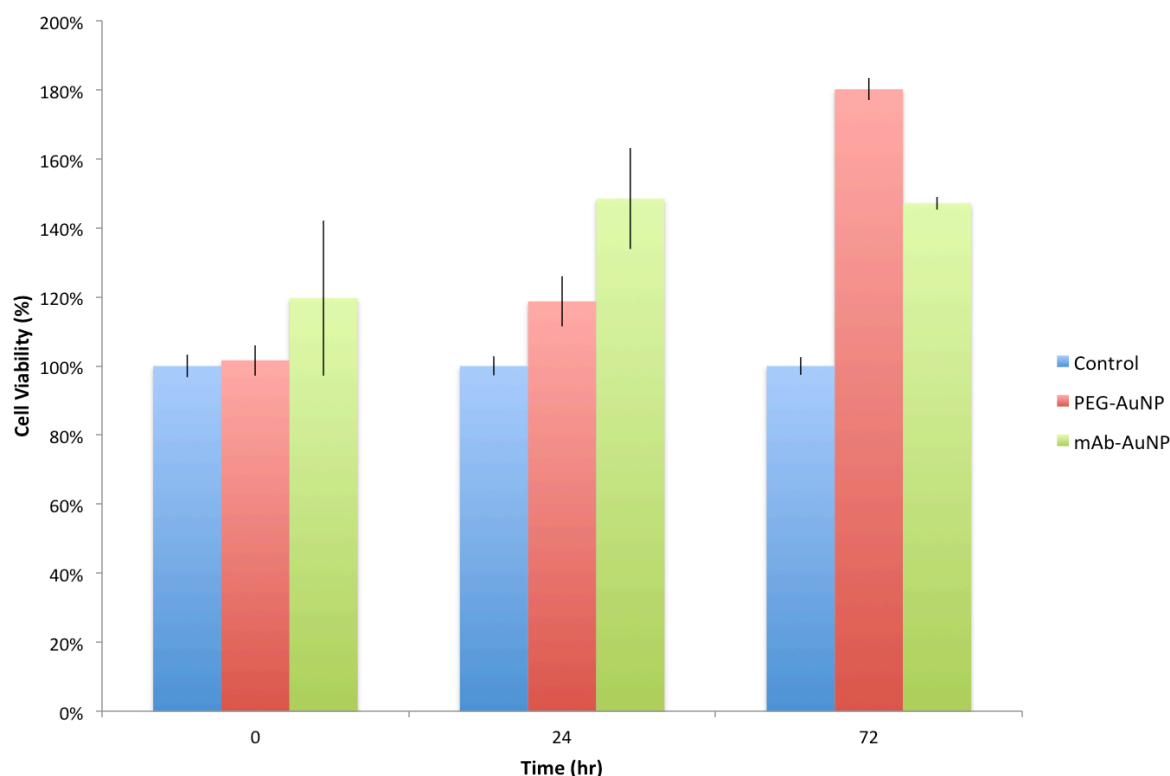


Figure 21. Cytotoxicity of thiol-PEG-azide gold nanoparticles and anti-CD47-AuNP *in vitro*. Cell viability measured using cell counting kit-8 according to manufacturer's protocol (Dojindo). *Homo sapiens* lung carcinoma cells (NCI-H2170). (n=1)

3.7 Future Direction

In this study we fail to show significant evidence for the successful conjugation of anti-CD47 antibody to gold nanoparticles via click chemistry. Future studies should be aimed to display significant conjugation by (1) increasing amount of anti-CD47 antibody, (2) altering the click chemistry protocol, or (3) utilizing an alternative analysis technique to test for the presence of antibody that is not dependent on the Fc region of the antibody. Once successful conjugation is achieved, future endeavors should be targeted to assess the final product's therapeutic effect on cancer cells in the presence of macrophages. The first step is an *in vitro* phagocytosis assay.¹³ Our hypothesis is that the anti-CD47-AuNP product should show comparable effectiveness in inducing phagocytosis of cancer cells as the anti-CD47 antibodies alone. Such test would investigate if the conjugation of the antibodies to the nanoparticles inhibits the antibodies in any way, such as by blocking the antigen-binding site. Given the number and location of amine groups on the structure of the antibody with which the nanoparticles could attach that would not cause any detrimental effect to the antigen-binding site (Figure 18), it is unlikely this conjugation method would significantly decrease the antibodies effectiveness in binding to CD47 protein, but should be studied before proceeding to *in vivo* studies.

If the *in vitro* assay produces promising results, the next step would be to perform an *in vivo* study to assess the therapeutic effect of anti-CD47-AuNP in a mouse model. We hypothesis our final product will show significantly greater effectiveness in treating tumors *in vivo* than the antibody alone because of the directed delivery provided by the nanoparticles. The final product's size will cause it to experience EPR to tumors,¹⁹⁻²¹ effectively delivering a higher dose of the antibody treatment directly to the cancerous cells. Further studies can also be conducted into the optimal size of the gold nanoparticles and number of antibodies conjugated to each nanoparticle to best maximizes its therapeutic effect.

4. Conclusion

In this study we fail to show significant evidence in support of the successful conjugation of anti-CD47 antibody to gold nanoparticles via click chemistry. Dodecanethiolate gold nanoparticles were synthesized using the Brust method,¹ and characterized by ¹H NMR spectroscopy and dynamic light scattering. Subsequent bromoundecanethiol exchange was conducted,² followed by an azide substitution to produce azidoundecanethiolate gold nanoparticles,² also characterized by ¹H NMR spectroscopy and dynamic light scattering. A thiol-PEG-azide substitution was conducted on the dodecanethiolate gold nanoparticles to produce water-soluble azido-gold nanoparticles.^{50,51} An alkyne was attached to anti-CD47 antibody, followed by click chemistry of the functionalized anti-CD47 antibody to the water-soluble azido-gold nanoparticles.^{50,51} The efficacy of the conjugation was investigated by an ELISA assay and found to be statistically insignificant ($p < 0.05$) and the anti-CD47-AuNP conjugated product demonstrates no cytotoxic effect on cells *in vitro*.

Given anti-CD47 antibody's demonstrated therapeutic effect on cancer cells *in vivo*,¹³ we propose the investigation of the therapeutic effect of anti-CD47-AuNP as a cancer therapy agent. We hypothesize that given gold nanoparticles' demonstrated utility as a directed delivery system for drugs,¹⁵⁻¹⁸ anti-CD47-AuNP will be more effective than the nonspecific anti-CD47 antibody treatment alone in inducing phagocytosis of established tumor cells *in vivo*.

5. References

1. Brust, M.; Walker, M.; Bethell, D.; Schiffrin, D.; Whyman, R. Synthesis of thiol-derivatised gold nanoparticles in a two-phase Liquid-Liquid system. *Journal of the Chemical Society, Chemical Communications* **1994**, 7, 801-802.
2. Boisselier, E.; Salmon, L.; Ruiz, J.; Astruc, D. How to very efficiently functionalize gold nanoparticles by "click" chemistry. *Chemical Communications* **2008**, 5788-5790.
3. Wang, J.; Boriskina, S. V.; Wang, H.; Reinhard, B. M. Illuminating Epidermal Growth Factor Receptor Densities on Filopodia through Plasmon Coupling. *ACS Nano* **2011**, 5, 6619-6628.
4. Rong, G.; Reinhard, B. M. Monitoring the size and lateral dynamics of ErbB1 enriched membrane domains through live cell plasmon coupling microscopy. *PLoS One* **2012**, 7, e34175.
5. Shuptrine, C.; Surana, R.; Weiner, L. Monoclonal antibodies for the treatment of cancer. *Seminars in Cancer Biology* **2012**, 22, 3-13.
6. Xia, Y.; Pawar, R.; Nakouzi, A.; Herlitz, L.; Broder, A.; Liu, K.; Goilav, B.; Fan, M.; Wang, L.; Li, Q.; Casadevall, A.; Putterman, C. The constant region contributes to the antigenic specificity and renal pathogenicity of murine anti-DNA antibodies. *Journal of Autoimmunity* **2012**, 39, 398-411.
7. Sawicka, M.; Pawlikowski, J.; Wilson, S.; Ferdinando, D.; Wu, H.; Adams, P.; Gunn, D.; Parish, W. The Specificity and Patterns of Staining in Human Cells and Tissues of p16INK4a Antibodies Demonstrate Variant Antigen Binding. *PLoS One* **2013**, 8, e53313.
8. Sterzyńska, K.; Kempisty, B.; Zawierucha, P.; Zabel, M. Analysis of the specificity and selectivity of anti-EpCAM antibodies in breast cancer cell lines. *Folia Histochem Cytobiol* **2012**, 50, 534-541.
9. Baselga, J.; Norton, L.; Albanell, J.; Kim, Y.; Mendelsohn, J. Recombinant humanized anti-HER2 antibody (herceptin) enhances the antitumor activity of paclitaxel and doxorubicin against HER2/neu overexpressing human breast cancer xenografts. *Cancer Research* **1998**, 58, 2825-2831.
10. Di Gaetano, N.; Cittera, E.; Nota, R.; Vecchi, A.; Grieco, V.; Scanziani, E.; Botto, M.; Introna, M.; Golay, J. Complement activation determines the therapeutic activity of rituximab in vivo. *The Journal of Immunology* **2003**, 171, 1581-1587.
11. Musolino, A.; Naldi, N.; Bortesi, B.; Pezzuolo, D.; Capelletti, M.; Missale, G.; Laccabue, D.; Zerbini, A.; Camisa, R.; Bisagni, G.; Neri, T. M.; Ardizzoni, A. Immunoglobulin g fragment c receptor polymorphisms and clinical efficacy of trastuzumab-based therapy in patients with HER-2/neu-positive metastatic breast cancer. *Journal of Clinical Oncology* **2008**, 26, 1789-1796.
12. Albert, M. L.; Sauter, B.; Bhardwaj, N. Dendritic cells acquire antigen from apoptotic cells and induce class I- restricted CTLs. *Nature* **1998**, 392, 86-89.
13. Willingham, S.; Volkmer, J.; Gentles, A.; Sahoo, D.; Dalerba, P.; Mitra, S.; Wang, J.; Contreras-Trujillo, H.; Martin, R.; Cohen, J.; Lovelace, P.; Scheeren, F.; Chao, M.; Weiskopf, K.; Tang, C.; Volkmer, A.; Naik, T.; Storm, T.; Mosley, A.; Edris, B.; Schmid, S.; Sun, C.; Chua, M.; Murillo, O.; Rajendran, P.; Cha, A.; Chin, R.; Kim, D.; Adorno, M.; Raveh, T.; Tseng, D.; Jaiswal, S.; Enger, P.; Steinberg, G.; Li, G.; So, S.; Majeti, R.; Harsh, G.; Van de Rijn, M.; Teng, N.; Sunwoo, J.; Alizadeh, A.; Clarke, M.; Weissman, I. The CD47-signal regulatory protein alpha (SIRPα) interaction is a therapeutic target for human solid tumors. *Proceedings of the National Academy of Sciences* **2012**, 109, 6662-6667.

14. Willingham, S. B.; Volkmer, J. -.; Gentles, A. J.; Sahoo, D.; Dalerba, P.; Mitra, S. S.; Wang, J.; Contreras-Trujillo, H.; Martin, R.; Cohen, J. D.; Lovelace, P.; Scheeren, F. A.; Chao, M. P.; Weiskopf, K.; Tang, C.; Volkmer, A. K.; Naik, T. J.; Storm, T. A.; Mosley, A. R.; Edris, B.; Schmid, S. M.; Sun, C. K.; Chua, M. -.; Murillo, O.; Rajendran, P.; Cha, A. C.; Chin, R. K.; Kim, D.; Adorno, M.; Raveh, T.; Tseng, D.; Jaiswal, S.; Enger, P. Ø.; Steinberg, G. K.; Li, G.; So, S. K.; Majeti, R.; Harsh, G. R.; Van Rijn, M. D.; Teng, N. N. H.; Sunwoo, J. B.; Alizadeh, A. A.; Clarke, M. F.; Weissman, I. L. The CD47-signal regulatory protein alpha (SIRPa) interaction is a therapeutic target for human solid tumors. *Proceedings of the National Academy of Sciences* **2012**, *109*, 6662-6667.
15. Brannon-Peppas, L.; Blanchette, J. O. Nanoparticle and targeted systems for cancer therapy. *Advanced Drug Delivery Reviews* **2004**, *56*, 1649-1659.
16. Brigger, I.; Dubernet, C.; Couvreur, P. Nanoparticles in cancer therapy and diagnosis. *Advanced Drug Delivery Reviews* **2012**, *64*, 24-36.
17. Wilczewska, A.; Niemirowicz, K.; Markiewicz, K.; Markiewicz, K.; Car, H. Nanoparticles as drug delivery systems. *Pharmacological Reports* **2012**, *64*, 1020-1037.
18. Voliani, V.; Signore, G.; Nifosí, R.; Ricci, F.; Luin, S.; Beltram, F. Smart Delivery and Controlled Drug Release with Gold Nanoparticles: New Frontiers in Nanomedicine. *Recent Patents on Nanomedicine* **2012**, *2*.
19. Dreaden, E.; Austin, L.; Mackey, L.; El-Sayed, M. Size matters: gold nanoparticles in targeted cancer drug delivery. *Therapeutic Delivery* **2012**, *3*, 457-478.
20. Maeda, H. Tumor-Selective Delivery of Macromolecular Drugs via the EPR Effect: Background and Future Prospects. *Bioconjugate Chemistry* **2010**, *21*, 797-802.
21. Maeda, H.; Bharate, G. Y.; Daruwalla, J. Polymeric drugs for efficient tumor-targeted drug delivery based on EPR-effect. *European Journal of Pharmaceutics and Biopharmaceutics* **2009**, *71*, 409-419.
22. Mukherjee, P.; Bhattacharya, R.; Bone, N.; Lee, Y.; Patra, C.; Wang, S.; Lu, L.; Secreto, C.; Banerjee, P.; Yaszemski, M.; Kay, N.; Mukhopadhyay, D. Potential therapeutic application of gold nanoparticles in B-chronic lymphocytic leukemia (BCLL): enhancing apoptosis. *Journal of Nanobiotechnology* **2007**, *5*, 4.
23. American Cancer Society Global Cancer Facts & Figures 2nd Edition. (accessed 12/11, 2013).
24. American Cancer Society Current Grants by Cancer Type as of 3/1/13. (accessed 10/12, 2013).
25. National Cancer Institute National Cancer Institute Fact Sheet: Cancer Research Funding. (accessed October, 2013).
26. National Institutes of Health FACT SHEET - Cancer. **October 2010**.
27. Sudhakar, A. History of Cancer, Ancient and Modern Treatment Methods. *Journal of Cancer Science & Therapy* **2009**, *2*, 1-4.
28. Chaffer, C.; Weinberg, R. A Perspective on Cancer Cell Metastasis. *Science* **2011**, *331*, 1559-1564.
29. DeVita, V.; Chu, E. A History of Cancer Chemotherapy. *Cancer Research* **2008**, *68*, 8643-8653.
30. Kaiser, M.; Ellenberg, S. Pancreatic cancer: Adjuvant combined radiation and chemotherapy following curative resection. *Archives of Surgery* **1985**, *120*, 899-903.
31. Frei, E.; Eder, J. In *Combination Chemotherapy*; Holland-Frei Cancer Medicine, **2003**, 6.

32. Malhotra, V.; Perry, M. Classical Chemotherapy: Mechanisms, Toxicities and the Therapeutic Window. *Cancer Biology & Therapy* **2003**, *2*, 1-3.
33. Sawyers, C. Targeted cancer therapy. *Nature* **2004**, *432*, 294-297.
34. Aggarwal, S. Targeted cancer therapies. *Nature Reviews Drug Discovery* **2010**, *9*, 427-428.
35. Zoubir, M.; Tursz, M.; Ménard, C.; Zitvogel, L.; Chaput, N. Imatinib Mesylate (Gleevec®): Targeted Therapy Against Cancer with Immune Properties. *Endocrine, Metabolic & Immune Disorders* **2010**, *10*, 1-7.
36. Chen, X.; Liu, Y.; Røe, O.; Qian, Y.; Guo, R.; Zhu, L.; Yin, Y.; Shu, Y. Gefitinib or Erlotinib as Maintenance Therapy in Patients with Advanced Stage Non-Small Cell Lung Cancer: A Systematic Review. *PLoS One* **2013**, *8*, e59314.
37. Zeng, Z.; Lin, J.; Chen, J. Bortezomib for patients with previously untreated multiple myeloma: a systematic review and meta-analysis of randomized controlled trials. *Annals of Hematology* **2013**, *92*, 935-943.
38. Qu, Z.; Griffiths, G.; Wegener, W.; Chang, C. H.; Govindan, S.; Horak, I.; Hansen, H.; Goldenberg, D. Development of humanized antibodies as cancer therapeutics. *Methods* **2005**, *36*, 84-95.
39. Stern, M.; Herrmann, R. Overview of monoclonal antibodies in cancer therapy: present and promise. *Critical Reviews in Oncology/Hematology* **2005**, *54*, 11-29.
40. Chao, M.; Weissman, I.; Majeti, R. The CD47–SIRPα pathway in cancer immune evasion and potential therapeutic implications. *Current Opinion in Immunology* **2012**, *24*, 225-232.
41. Shuptrine, C.; Surana, R.; Weiner, L. Monoclonal antibodies for the treatment of cancer. *Seminars in Cancer Biology* **2012**, *22*, 3-13.
42. Hansel, T.; Kropshofer, H.; Singer, T.; Mitchell, J.; George, A. The safety and side effects of monoclonal antibodies. *Nature Reviews Drug Discovery* **2010**, *9*, 325-338.
43. Yuan, F.; Dellian, M.; Fukumura, D.; Leunig, M.; Berk, D.; Torchilin, V.; Jain, R. K. Vascular Permeability in a Human Tumor Xenograft: Molecular Size Dependence and Cutoff Size. *Cancer Research* **1995**, *55*, 3752-3756.
44. Yuan, F.; Leunig, M.; Huang, S.; Berk, D.; Papahadjopoulos, D.; Jain, R. Microvascular Permeability and Interstitial Penetration of Sterically Stabilized (Stealth) Liposomes in a Human Tumor Xenograft. *Cancer Research* **1994**, *54*, 3352-3356.
45. Unezaki, S.; Maruyama, K.; Hosoda, J.; Nagae, I.; Koyanagi, Y.; Nakata, M.; Ishida, O.; Iwatsuru, M.; Tsuchiya, S. Direct measurement of the extravasation of polyethyleneglycol-coated liposomes into solid tumor tissue by in vivo fluorescence microscopy. *International Journal of Pharmaceutics* **1996**, *144*, 11-17.
46. Terentyuk, G.; Maslyakova, G.; Suleymanova, L.; Khlebtsov, B.; Kogan, B.; Akchurin, G.; Shantrocha, A.; Maksimova, I.; Khlebtsov, N.; Tuchin, V. Circulation and distribution of gold nanoparticles and induced alterations of tissue morphology at intravenous particle delivery. *Journal of Biophotonics* **2009**, *2*, 292-302.
47. Qian, X.; Peng, X.; Ansari, D.; Yin-Goen, Q.; Chen, G.; Shin, D.; Yang, L.; Young, A.; Wang, M.; Nie, S. In vivo tumor targeting and spectroscopic detection with surface-enhanced Raman nanoparticle tags. *Nature Biotechnology* **2008**, *26*, 83-90.
48. Thorek, D.; Elias, D.; Tsourkas, A. Comparative analysis of nanoparticle-antibody conjugations: carbodiimide versus click chemistry. *Molecular Imaging* **2009**, *8*, 221-229.
49. Uttamapinant, C.; Tangpeerachaikul, A.; Grecian, S.; Clarke, S.; Singh, U.; Slade, P.; Gee, K.; Ting, A. Fast, Cell-Compatible Click Chemistry with Copper-Chelating Azides for Biomolecular Labeling. *Angewandte Chemie International Edition* **2012**, *51*, 5852-5856.

50. Rong, G.; Reinhard, B. M. Monitoring the size and lateral dynamics of ErbB1 enriched membrane domains through live cell plasmon coupling microscopy. *PLoS One* **2012**, *7*, e34175.
51. Wang, J.; Boriskina, S. V.; Wang, H.; Reinhard, B. M. Illuminating Epidermal Growth Factor Receptor Densities on Filopodia through Plasmon Coupling. *ACS Nano* **2011**, *5*, 6619-6628.
52. Zhou, M.; Wang, B.; Rozynek, Z.; Xie, Z.; Fossum, J. O.; Yu, X.; Raaen, S. Minute synthesis of extremely stable gold nanoparticles. *Nanotechnology* **2009**, *20*, 505606-4484/20/50/505606. Epub 2009 Nov 19.
53. Hardy, E.; Kamphuis, T.; Japaridze, A.; Wilschut, J. C.; Winterhalter, M. Nanoaggregates of micropurified lipopolysaccharide identified using dynamic light scattering, zeta potential measurement, and TLR4 signaling activity. *Anal. Biochem.* **2012**, *430*, 203-213.
54. Khlebtsov, N.; Dykman, L. Biodistribution and toxicity of engineered gold nanoparticles: a review of in vitro and in vivo studies. *Chem. Soc. Rev.* **2011**, *40*, 1647-1671.
55. Taylor, U.; Barchanski, A.; Garrels, W.; Klein, S.; Kues, W.; Barcikowski, S.; Rath, D. Toxicity of gold nanoparticles on somatic and reproductive cells. *Adv. Exp. Med. Biol.* **2012**, *733*, 125-133.
56. Zhang, X.; Wu, D.; Shen, X.; Liu, P.; Yang, N.; Zhao, B.; Zhang, H.; Sun, Y.; Zhang, L.; Fan, F. Size-dependent in vivo toxicity of PEG-coated gold nanoparticles. *Int J Nanomedicine* **2011**, *6*, 2071-2081.
57. Thermo Scientific Antibody Labeling: Antibody-Modification Sites. (<http://www.piercenet.com/2013>).
58. Le, H. T.; Jang, J. G.; Park, J. Y.; Lim, C. W.; Kim, T. W. Antibody functionalization with a dual reactive hydrazide/click crosslinker. *Anal. Biochem.* **2013**, *435*, 68-73.
59. Robardet, E.; Andrieu, S.; Rasmussen, T. B.; Dobrostana, M.; Horton, D. L.; Hostnik, P.; Jaceviciene, I.; Juhasz, T.; Muller, T.; Mutinelli, F.; Servat, A.; Smreczak, M.; Vanek, E.; Vazquez-Moron, S.; Cliquet, F. Comparative assay of fluorescent antibody test results among twelve European National Reference Laboratories using various anti-rabies conjugates. *J. Virol. Methods* **2013**, *191*, 88-94.